



City Research Online

City, University of London Institutional Repository

Citation: Lockett, R. D. & Robertson, G. (2014). A Dynamical Systems Analysis of Methanol-Air Auto-Ignition. ., doi: 10.13140/2.1.2907.1369

This is the draft version of the paper.

This version of the publication may differ from the final published version.

Permanent repository link: <https://openaccess.city.ac.uk/id/eprint/8190/>

Link to published version: <https://doi.org/10.13140/2.1.2907.1369>

Copyright: City Research Online aims to make research outputs of City, University of London available to a wider audience. Copyright and Moral Rights remain with the author(s) and/or copyright holders. URLs from City Research Online may be freely distributed and linked to.

Reuse: Copies of full items can be used for personal research or study, educational, or not-for-profit purposes without prior permission or charge. Provided that the authors, title and full bibliographic details are credited, a hyperlink and/or URL is given for the original metadata page and the content is not changed in any way.

A Dynamical Systems Analysis of Methanol-Air Auto-Ignition

¹R.D. Lockett, ²G.N. Robertson

¹School of Engineering and Mathematical Sciences, The City University,
Northampton Square, London, EC1V 0HB, United Kingdom.

²Department of Physics, University of Cape Town, Rondebosch 7700,
Republic of South Africa.

Corresponding Author: R.D. Lockett

Email: r.d.lockett@city.ac.uk

Tel. 44 (0) 207 040 8812

Fax. 44 (0) 207 040 8566

Abstract

Dynamical systems analysis was employed as an alternative investigative tool to conventional reaction path analysis and sensitivity analysis in methanol-air auto-ignition, in which the non-linear chemical rate equations describing a homogeneous, methanol-air auto-ignition system were linearised. The resultant system of linear, inhomogeneous differential equations were solved analytically using an eigen-mode analysis. The numerically determined solution to the non-linear auto-ignition trajectory was employed to determine the local analytic behaviour for a number of regular points along the solution trajectory to equilibrium. The solution trajectory was found to qualitatively change three times, thereby defining four different regions in the time and temperature domain. The dominant eigen-mode solutions were expressed in terms of dominant reactions at regular intervals along the solution path, revealing the dominant local chemistry. The solution trajectory was dominated by four explosive modes in the first, low temperature region ($T < 1,090$ K). Two dominant explosive modes coupled to form an explosive, oscillating mode in the second region ($1,090$ K $< T < 1,160$ K). In the third region ($1,160$ K $< T < 2,000$ K), the explosive, oscillating mode changed to a decaying, oscillating mode. The changes in the low temperature region of the solution trajectory were found to be associated with the critical points in the evolution of the branching agent (hydrogen peroxide) concentration. The third qualitative change occurred at $T \sim 2,000$ K, when the dominant decaying, oscillating mode describing methanol and formaldehyde oxidation to carbon monoxide collapsed, to be replaced with real, decaying modes (proper stable nodes) describing the wet oxidation of carbon monoxide to carbon dioxide, and its reverse reaction, together with the high temperature formation of water and other equilibrium products.

Keywords

Dynamical Systems Analysis, Auto-ignition, Bifurcation, Chemical Kinetics, Eigenmode Analysis, Chemical Explosion, Branching, Thermal Explosion.

1. Introduction

It is a common practice in the study of systems of non-linear differential equations to linearise the set of equations about various points along the solution trajectory (usually in the neighbourhood of a local equilibrium point), and then, wherever possible, solve for the linearised system. These linearised solutions are then first order approximations to the true solution of the problem, and are generally used to study the qualitative behaviour of the non-linear system at the specified points along the solution trajectory. This approach forms the basis of a dynamical systems analysis of a non-linear dynamical system [1, 2].

Furthermore, the linearised mathematical solution at regular points along the solution trajectory of a real, non-linear dynamical system can be decomposed into terms of real eigen-modes or complex conjugate pairs of eigen-modes. The full linear solution can then be expressed in terms of a sum of one- and two-dimensional eigen-mode solutions. The eigen-modes have eigenvalues that are either real and positive (explosive modes), real and negative (decaying modes), complex with positive real parts (explosive, oscillatory modes), complex with negative real parts (decaying, oscillatory modes), or imaginary.

Several methods of dynamical systems analysis have been employed in theoretical and numerical research in combustion. K. Chinnick *et al* [3] used a linearisation technique in studying oscillatory reaction behaviour in H_2/O_2 systems. This study was conducted analytically using a simplified H_2/O_2 reaction mechanism. They were able to derive explicit expressions defining the critical ignition boundary criteria and the conditions for oscillatory ignition.

On the other hand, Maas and Pope [4] have used qualitative dynamical methods as a means of determining how flame chemical kinetics can be simplified. They showed that the linearised time development of flame chemistry can be closely approximated by a subspace of the composition space, where the subspace is defined as that in which all movements of the chemistry correspond to slower time scales. This subspace is determined by finding the points in the composition space that are in equilibrium with respect to the fastest time scales of the chemical system. The linear analysis was then generalised to the full non-linear problem. They were able to demonstrate the method successfully for a CO/H₂/air system, reducing the system to one and two-dimensional manifolds in the reaction space, and comparing the results with conventional reduced mechanisms. Maas, Pope and others have since applied this technique to chemical mechanism reduction in complex flame chemistry successfully [5 – 8].

The Computational Singular Perturbation (CSP) method of mechanism analysis and reduction has been developed by Lam and Goussis [9 – 11]. This method involves utilizing the eigenvectors obtained from the diagonalisation of the linearised rate equation Jacobian as a preferred set of basis vectors to identify the fast chemistry manifold (near-equilibrium processes), and the slow chemistry manifold (time-dependent processes) imbedded in the solution manifold. The eigenvalues obtained from the diagonal Jacobian define the different time scales associated with the chemical kinetic solution trajectory, and are employed to discriminate between the slow chemistry manifold and the fast chemistry manifold. The eigenvectors associated with the slow manifold are then used to determine the tangent space to the slow chemistry manifold. The tangent space is then employed to achieve the reduction of

the chemical mechanism. The methodology has been further developed, refined, and employed by them and others [12 – 14].

As a result, the methods of dynamical systems analysis are often employed in the canonical reduction of combustion mechanisms. However, the methodology can also be employed to provide new insights into the evolution of chemically explosive combustion systems, to be used, either together with, or as an alternative to, reaction path analysis and sensitivity analysis. Natural applications of this methodology include explosion limits, ignition processes, engine auto-ignition and HCCI combustion.

The mathematical method presented here is very similar to that of the original work of Maas and Pope [4], and Lam and Goussis [9], but was developed independently of them, at around the same time [15]. The fundamental difference between this analysis, and that of Maas and Pope, is that this was developed in order to provide a new and alternative insight into chemically explosive systems. The expectation was that, in a chemically explosive system described by branching, only a small number of independent eigen-modes would dominate the solution trajectory. Low temperature chemical branching and high temperature recombination is of central importance in understanding auto-ignition, and can then be understood in terms of the development of these eigen-modes, rather than in terms of a numerical solution to a large system of coupled reaction equations. Dynamical systems analysis of auto-ignition is expected to provide a more intuitive explanation of chemical branching, propagation and equilibrium termination than conventional reaction path analysis (RPA) and/or sensitivity analysis (SA), which will be discussed in detail later.

Section 2 contains a presentation of a number of standard methods employed in the analysis of combustion mechanisms. These include the quasi-steady state

approximation (QSSA), the method of partial equilibrium (PEA), reaction path analysis (RPA), and sensitivity analysis (SA). Section 2 is provided in order to contrast the results of dynamical systems analysis with the more conventional methods of chemical mechanism analysis.

In addition to the other conventional methods of mechanism analysis (Quasi-Steady State Approximation (QSSA), Partial Equilibrium Assumption (PEA), RPA, and SA), high activation energy asymptotic analysis has been employed successfully in the course of investigating the basic structure of flames subject to single step chemistry [16, 17], the detailed structure of the relatively cool induction region of hydrogen-oxygen detonation waves [18], and a number of other combustion applications [19, 20].

The dynamical systems analysis contained in this paper was applied to the modeling study of methanol auto-ignition in a methanol-fuelled internal combustion engine performed by Driver *et al.* [21]. The physical model to be explored was how the cylinder end-gas (the unburned mixture ahead of the flame front) had its enthalpy raised by cylinder and flame front compression, and heat transfer, until auto-ignition, followed by a comprehensive examination of the branching and thermal chemistry involved in auto-ignition.

The explosive chemical system subjected to analysis was a homogeneous methanol/air mixture subjected to a measured, temperature-pressure-volume history until shortly before the mixture became explosive. Following the last of the temperature measurements, the mixture was assumed to be subject to adiabatic compression until and through the calculated chemical and thermal explosion. For the experimental details of the temperature and pressure measurements in the engine, the

reader should refer to reference [22], and for the modeling details of the auto-ignition chemistry, the reader should refer to references [21] and [23].

2. An Introduction to Mechanism Analysis

2.1 Quasi-Steady State Approximation (QSSA)

A simple reaction sequence, consisting of two elementary reaction steps, will be employed to illustrate the quasi-steady state approximation. The reaction sequence



subject to initial conditions $[A](t_0) = A_0$, $[B](t_0) = 0$, $[C](t_0) = 0$, and $[D](t_0) = 0$, has an exact analytic solution for the time-dependent species concentrations:

$$[A](t) = A_0 e^{-k_1(t-t_0)}, \quad (1)$$

$$[B](t) = A_0 \frac{k_1}{k_1 - k_2} \left(e^{-k_2(t-t_0)} - e^{-k_1(t-t_0)} \right), \quad (2)$$

$$[C](t) = [D](t) = A_0 \left(1 - \frac{k_1 e^{-k_2(t-t_0)}}{k_1 - k_2} + \frac{k_2 e^{-k_1(t-t_0)}}{k_1 - k_2} \right). \quad (3)$$

If it is now assumed that species B is very reactive in forming C and D ($k_2 \gg k_1$), then the rate of consumption of species B is approximately equal to the rate of formation of species B . This condition defines the quasi-steady state approximation, which is then expressed as

$$\frac{d[B]}{dt} = k_1[A] - k_2[B] \approx 0. \quad (4)$$

Solving for $[B](t)$, $[C](t)$, and $[D](t)$ produces the solutions

$$[B](t) = \frac{k_1 A_0}{k_2} e^{-k_1(t-t_0)}, \quad (5)$$

$$[C](t) = [D](t) = A_0(1 - e^{-k_1(t-t_0)}). \quad (6)$$

A comparison of the exact solutions and the approximate solutions obtained using the quasi-steady state approximation above shows that the approximate solution is obtained directly from the exact solution when $k_2 \gg k_1$, and $t - t_0 \gg 1/k_2$.

A classic example of the application of the quasi-steady state approximation which is widely taught in combustion courses involves the derivation of the overall reaction rate for the oxidation of hydrogen in bromine to form hydrogen bromide [24, 25].

The proposed mechanism for the oxidation of hydrogen in bromine is



Using the quasi-steady state assumption, the rate laws for the intermediates H and Br are

$$\begin{aligned}\frac{d[Br]}{dt} &= 2k_1[Br_2][M] + k_3[H][HBr] + k_4[H][Br_2] - k_2[Br][H_2] - 2k_5[Br]^2[M] \approx 0 \\ \frac{d[H]}{dt} &= k_2[Br][H_2] - k_3[H][HBr] - k_4[H][Br_2] \approx 0\end{aligned}\quad (7)$$

Therefore $[H] = \frac{k_2[Br][H_2]}{k_3[HBr] + k_4[Br_2]}$. Summation of these two equations produces

$$[Br] = \sqrt{\frac{k_1[Br_2]}{k_5}}. \text{ Hence the rate law for the formation of hydrogen bromide is}$$

$$\frac{d[HBr]}{dt} = k_2[Br][H_2] + k_4[H][Br_2] - k_3[H][HBr] = \frac{2k_2\sqrt{\frac{k_1[Br_2]}{k_5}}[H_2]}{1 + \frac{k_3[HBr]}{k_4[Br_2]}} \quad (8)$$

2.2 Partial Equilibrium Assumption (PEA)

An example of the partial equilibrium assumption can be found in high temperature hydrogen-oxygen combustion ($T > 2000\text{K}$) [26]. A modern hydrogen-oxygen combustion mechanism can be employed to show that the following forward and reverse reactions



are very fast at high temperatures ($T > 2000\text{K}$). Under these conditions, a partial equilibrium is said to exist for these three reactions. Hence

$$k_1[H][O_2] = k_2[OH][O] \quad (9)$$

$$k_3[H_2][O] = k_4[OH][H] \quad (10)$$

$$k_5[H_2][OH] = k_6[H_2O][H]. \quad (11)$$

The intermediate species concentrations can then be expressed in terms of the major species concentrations:

$$\begin{aligned} [H] &= \sqrt{\frac{k_1 k_3 k_5^2 [H_2]^3 [O_2]}{k_2 k_4 k_6^2 [H_2O]^2}} \\ [O] &= \frac{k_1 k_5 [H_2] [O_2]}{k_2 k_6 [H_2O]} \\ [OH] &= \sqrt{\frac{k_1 k_3}{k_2 k_4} [H_2] [O_2]} \end{aligned} \quad (12)$$

2.3 Reaction Path Analysis (RPA)

During the numerical integration of a set of rate equations in order to obtain the solution trajectory, the mechanism itself can be subjected to a local analysis in order to discover the relationship between individual reactions and the rate of formation and consumption of the active chemical species. This analysis constitutes the basis for a local reaction path analysis [26].

The results of the local reaction path analysis are normally presented in the form of a table, providing the relative rates of formation and consumption of species by the reactions constituting the mechanism. The table is normally determined for each point along the solution trajectory. Table 1 below shows the format of such a table, and the type of information provided.

(Please insert Table 1 here.)

Integrating the local reaction path over the time domain from initiation to completion defines an integral or global reaction path analysis [26]. This analysis provides the dominant reaction paths for the entire combustion process under investigation. The results of an integral path analysis are normally presented in the form of a flowchart. Figure 1 shows such a flowchart, indicating the reaction flow for the explosive oxidation of methanol in air, initiated from an intermediate temperature ($T \sim 1,100$ K).

(Please insert Figure 1 here.)

2.4 Sensitivity Analysis (SA)

The chemical rate law describing the rate of change of concentration of chemical species with time, temperature and pressure, can be expressed in vector form in the following way:

$$\frac{d}{dt} \mathbf{y}(t) = \mathbf{A}(T) \cdot \mathbf{y} + \mathbf{B}(T) : \mathbf{y}\mathbf{y} + \mathbf{C}(T) \vdash \mathbf{y}\mathbf{y}\mathbf{y}, \quad (13)$$

where $\mathbf{y}(t)$ is the species concentration vector, and $\mathbf{A}(T)$, $\mathbf{B}(T)$, and $\mathbf{C}(T)$ are two-dimensional, three dimensional, and four dimensional matrices respectively, containing in turn molecular fission reaction rate coefficients, bi-molecular collision rate coefficients, and termolecular collision rate coefficients.

Suppose that a number of reaction rate coefficients describing reactions comprising the combustion mechanism are ill-defined (this is usually the case in fully detailed combustion mechanisms). Sensitivity analysis of the combustion mechanism aims to provide quantitative information on the relative dependence of species concentrations on reaction rate coefficients. Applying sensitivity analysis to a combustion mechanism enables the determination of the dominant elementary reactions determining the solution trajectory.

The relative sensitivity of the i 'th species concentration (y_i) to a variation in reaction rate coefficient k_j for the j 'th reaction is defined by S_{ij} [27], where

$$S_{ij} = \frac{k_j}{y_i} \frac{\partial y_i}{\partial k_j} = \frac{\partial \ln y_i}{\partial \ln k_j} . \quad (14)$$

As an example, this definition of the relative sensitivity will be applied to the simple reaction sequence discussed in Section 2.1 above (Reaction Sequence A). The relative sensitivity of species 3 (species C) to reaction rate coefficients k_1 and k_2 is then given by

$$\begin{aligned} S_{31} &= \frac{A_0 k_1 k_2}{[C](k_1 - k_2)^2} \left[((k_2 - k_1)t - 1)e^{-k_1 t} + e^{-k_2 t} \right] \\ S_{32} &= \frac{A_0 k_1 k_2}{[C](k_1 - k_2)^2} \left[((k_1 - k_2)t - 1)e^{-k_2 t} + e^{-k_1 t} \right] . \end{aligned} \quad (15)$$

Following on from the above example ($k_2 \gg k_1$), $S_{31} \rightarrow 1$ as $t \rightarrow \infty$, and $S_{32} \rightarrow 0$ as $t \rightarrow \infty$. This result identifies that the product species C has a large relative sensitivity

to the slow, rate limiting reaction rate of $A \rightarrow B$, and small relative sensitivity to the fast reaction rate of $B \rightarrow C + D$.

Figure 2 shows the relative sensitivity of the various species involved in the auto-ignition of methanol in air, taken from reference [21].

(Please insert Figure 2 here.)

3. Derivation of the Linear Mode Analysis

The system of reaction equations are linearised in the following way. The species concentration vector $\mathbf{y}(t)$ has vector elements denoted by $y_i(t)$, $i \in [1, 2, 3, \dots, N]$, where N is the number of atomic and molecular species in the complete chemical mechanism. $\mathbf{y}(t)$ evolves according to the system of equations

$$\frac{d}{dt}\mathbf{y}(t) = \mathbf{A}(T)\cdot\mathbf{y} + \mathbf{B}(T):\mathbf{y}\mathbf{y} + \mathbf{C}(T):\mathbf{y}\mathbf{y}\mathbf{y}. \quad (16)$$

The two-dimensional matrix \mathbf{A} contains temperature dependent rate coefficients for all of the uni-molecular decomposition reactions in the mechanism. The matrix elements of \mathbf{A} are denoted by A_{ij} , $i, j \in [1, 2, 3, \dots, N]$. The three-dimensional matrix \mathbf{B} contains temperature dependent rate coefficients for all of the bimolecular reactions in the mechanism. The matrix elements of \mathbf{B} are denoted by B_{ijk} , $i, j, k \in [1, 2, 3, \dots, N]$. The four-dimensional matrix \mathbf{C} contains temperature dependent rate coefficients for all of the termolecular reactions in the mechanism. The matrix elements of \mathbf{C} are denoted by C_{ijkl} , $i, j, k, l \in [1, 2, 3, \dots, N]$.

If the species concentration solution vector $\mathbf{y}(t)$ is expanded about some regular point in the solution trajectory $\mathbf{y}(t_0)$, then the concentration displacement vector from that regular point $\mathbf{x}(t)$ can be defined as $\mathbf{x}(t) = \mathbf{y}(t) - \mathbf{y}(t_0)$.

The equation for $\mathbf{x}(t)$ can be expressed in terms of the i 'th element of the vector, which is given by

$$\begin{aligned} \frac{dx_i}{dt} = & \sum_{j=1}^N A_{ij} (x_j + y_j(t_0)) + \sum_{j=1}^N \sum_{k=1}^N B_{ijk} (x_j + y_j(t_0))(x_k + y_k(t_0)) \\ & + \sum_{j=1}^N \sum_{k=1}^N \sum_{l=1}^N C_{ijkl} (x_j + y_j(t_0))(x_k + y_k(t_0))(x_l + y_l(t_0)) \end{aligned} \quad (17)$$

The non-linear terms in equation (17) above involve sums over the product terms $x_j x_k$ and $x_j x_k x_l$.

Equation (17) is linearised by ignoring terms that are quadratic and cubic in the concentration displacement vector \mathbf{x} . This yields the linearised equation for the i 'th component of the vector \mathbf{x} .

$$\begin{aligned} \dot{x}_i = \frac{dx_i}{dt} = & \sum_{j=1}^N A_{ij} y_j(t_0) + \sum_{j=1}^N \sum_{k=1}^N B_{ijk} y_j(t_0) y_k(t_0) + \sum_{j=1}^N \sum_{k=1}^N \sum_{l=1}^N C_{ijkl} y_j(t_0) y_k(t_0) y_l(t_0) \\ & + \sum_{j=1}^N A_{ij} x_j + \sum_{j=1}^N \sum_{k=1}^N [(B_{ijk} + B_{ikj}) y_k(t_0)] x_j + \sum_{j=1}^N \sum_{k=1}^N \sum_{l=1}^N [(C_{ijkl} + C_{ikjl} + C_{ilkj}) y_k(t_0) y_l(t_0)] x_j \end{aligned} \quad (18)$$

Equation (18) can be re-written in a simpler form

$$\dot{x}_i = M_i + \sum_{j=1}^N K_{ij} x_j \quad (19)$$

Equation (19) can be expressed in vector form

$$\frac{d}{dt} \mathbf{x} = \mathbf{K} \cdot \mathbf{x} + \mathbf{M}. \quad (20)$$

An alternative formulation of the problem expressed above can be obtained through a Taylor series expansion of the concentration vector $\mathbf{y}(t)$ about a regular point in the trajectory $\mathbf{y}(t_0)$.

$$\frac{d}{dt} \mathbf{y}(t) = \mathbf{A}(T) \cdot \mathbf{y} + \mathbf{B}(p, T) : \mathbf{y}\mathbf{y} + \mathbf{C}(p, T) : \mathbf{y}\mathbf{y}\mathbf{y} = \mathbf{f}(\mathbf{y}). \quad (21)$$

The local behaviour of the concentration vector $\mathbf{y}(t)$ in the neighborhood of a regular point in the trajectory $\mathbf{y}(t_0)$ can be determined by approximating the vector \mathbf{f} in the neighborhood of $\mathbf{y}(t_0)$. The first order approximation is

$$\mathbf{f}(\mathbf{y}_0 + \mathbf{d}\mathbf{y}) = \mathbf{f}(\mathbf{y}_0) + \mathbf{K} \cdot \mathbf{d}\mathbf{y} \quad (22)$$

where \mathbf{K} is the Jacobian matrix obtained from $\mathbf{f}(\mathbf{y})$ [4]. The first order approximation leads to the linear differential equations above (equations (19) and (20)).

Equations (19) and (20) define a system of coupled first order linear differential equations, with initial conditions $\mathbf{x}(t_0) = 0$. As long as the matrix \mathbf{K} can be diagonalised, the general solution for equation (20) above is

$$\mathbf{x}(t) = \mathbf{Q} \cdot e^{\gamma(t-t_0)} \cdot \mathbf{C} - \mathbf{Q} \cdot \gamma^{-1} \cdot \mathbf{Q}^{-1} \cdot \mathbf{M} \quad (23)$$

where \mathbf{Q} is the matrix of eigenvectors of matrix \mathbf{K} , $\boldsymbol{\gamma}$ is a diagonal matrix with the diagonal elements given by the eigenvalues of matrix \mathbf{K} , and $e^{\boldsymbol{\gamma}(t-t_0)}$ is the diagonal matrix

$$e^{\boldsymbol{\gamma}(t-t_0)} = \begin{pmatrix} e^{\gamma_1(t-t_0)} & 0 & 0 & \dots \\ 0 & e^{\gamma_2(t-t_0)} & 0 & \dots \\ 0 & 0 & e^{\gamma_3(t-t_0)} & \dots \\ \vdots & \vdots & \vdots & \ddots \end{pmatrix} \quad (24)$$

It is believed that the linearised matrix \mathbf{K} , derived from a realistic, detailed chemical mechanism where all elements of the matrix are real, and all species concentrations are linearly independent of all other species concentrations, is diagonalizable at all regular points along the solution trajectory except at the final equilibrium point, and the eigenvalues of \mathbf{K} remain distinct.

Applying the initial conditions yields the exact solution

$$\mathbf{x}(t) = \mathbf{Q} \cdot (e^{\boldsymbol{\gamma}(t-t_0)} - \boldsymbol{\delta}) \cdot \boldsymbol{\gamma}^{-1} \cdot \mathbf{Q}^{-1} \cdot \mathbf{M} \quad (25)$$

The linearised solution for $\mathbf{x}(t)$ is in the form of an eigenvalue-eigenvector decomposition of matrix \mathbf{K} , involving the vector \mathbf{M} .

In order to find the projection of the solution vector $\mathbf{x}(t)$ onto the eigenvectors, we write

$$\mathbf{x}(t) = \mathbf{Q} \cdot \mathbf{a}(t) \quad (26)$$

$\mathbf{a}(t)$ is the time dependent projection of the solution vector $\mathbf{x}(t)$ onto the eigenvectors, and is found by pre-multiplying the above equation by \mathbf{Q}^{-1} to give

$$\mathbf{a}(t) = \mathbf{Q}^{-1} \cdot \mathbf{x}(t) \quad (27)$$

yielding

$$\mathbf{a}(t) = (e^{\gamma(t-t_0)} - \delta) \cdot \gamma^{-1} \cdot \mathbf{Q}^{-1} \cdot \mathbf{M} \quad (28)$$

Mathematical systems of this sort are dynamic in the sense that the linearised solution derived above reflects not only the reaction chemistry, but also the response of the system to changes in the state variables, such as temperature, pressure and volume. A study of the evolution of the eigenvalues, eigenvectors and consequent solution vector therefore provides important information on the qualitative behaviour of the system. The dominant modes of the system are those whose rates of production of species are largest.

In mathematical systems of this kind, the eigen-mode solutions that dominate the solution trajectory may abruptly change their analytic behaviour. The system is then said to have undergone a bifurcation at this point. This change in analytic behaviour reveals a qualitative change in the evolution of the system. Bifurcations are identified as follows: no functional mapping exists to map the form of the solution prior to the bifurcation to the solution after the bifurcation. Pseudo-bifurcations occur when the solutions change structure, but a functional mapping can be found to map the solution prior to the pseudo-bifurcation to the solution after the pseudo-bifurcation.

By examining closely the detailed mechanism around the bifurcation and pseudo-bifurcation points, the reasons for the bifurcations, and hence the source of the corresponding change in the chemistry, can be revealed.

Eigen-mode rates of formation and consumption at regular points along the solution trajectory are derivable from Equation (28) in the form

$$\mathbf{c}(t) = \frac{d}{dt} \mathbf{a}(t) = \mathbf{Q}^{-1}(t) \cdot \mathbf{M}(t) \quad (29)$$

The eigen-mode rates of formation and consumption for the i 'th chemical species in the system can be expressed in the form $c_i(t) = \sum_j Q_{ij}^{-1}(t) M_j(t)$.

4. Programming Features

The original modeling was performed on a personal computer, using Warnatz's HOMREACT program [28], based on Deuflhard's numerical integrator LIMEX [29]. The modeling was performed using a core set of 188 reactions involving 21 chemical species extracted from the mechanism proposed by Grotheer *et al* [23]. This mechanism was employed to calculate the methanol/air auto-ignition process, which was then compared against the auto-ignition calculation involving the full mechanism [21]. There were no significant differences found. Furthermore, for purposes of comparison, the analysis presented here was repeated using the Norton and Dryer mechanism [30], and the later Held and Dryer mechanism [31]. There were no significant differences regarding the predicted auto-ignition trajectories obtained from the various mechanisms, nor the mathematical behaviour of the various solutions.

A FORTRAN program called CHEMMODE was written to calculate numerical expressions for $x(t)$ and $a(t)$. The output of HOMREACT includes local concentrations, temperatures, pressures, rate coefficients, and reaction stoichiometric coefficients at regular points along the solution trajectory. CHEMMODE reads in this data, prepares the Jacobian matrix \mathbf{K} and the vector \mathbf{M} , and then diagonalises \mathbf{K} . The elements of \mathbf{K} are all real. Therefore, the eigenvalues and eigenvector elements must be real, or complex conjugate pairs, in order for $x(t)$ to have real elements.

The routine used to diagonalise the Jacobian matrix \mathbf{K} first balanced the matrix, followed by a similarity transformation to upper Hessenberg form, analogous to Gaussian elimination with pivoting. The routine then used a QR algorithm with shifts and Gaussian elimination with pivoting to find the eigenvalues and eigenvectors respectively.

5. Eigen-Mode Analysis of Methanol/Air Auto-ignition

5.1 Preliminary Remarks

This section discusses the mathematical structure of the dominant eigen-modes along the solution trajectory of the methanol-air auto-ignition system, and the chemistry that results. In the following analysis, the eigen-mode rates of formation and consumption are presented as forward reactions with the relevant elements of the eigenvectors altered to achieve a normalized unit stoichiometric coefficient for the most important reactant. These reactions (derived from the eigenvectors) form the basis for a rigorous decomposition and analysis of the auto-ignition system. The γ_i represent the eigenvalues of the dominant eigen-modes presented, and the c_i are the

rates of production of species associated with the specified eigen-mode at time t_0 , and are given by $c_i = \sum_j Q_{ij}^{-1} M_j$.

Figure 3 shows the evolution of the major species concentrations and the temperature during auto-ignition [21]. Figure 4 shows the evolution of the intermediate species concentrations and the temperature during auto-ignition [21]. The three bifurcations are shown on the graphs occurring at the times specified by the three vertical lines crossing the time axis.

(Please insert Figure 3 here.)

(Please insert Figure 4 here.)

5.2 Eigen-Mode Analysis

In summary, the solution trajectory of the auto-ignition system bifurcates three times during the course of the reaction. During the first part of the branching reaction, the dominant eigen-modes are explosive modes (the dominant modes have real, positive eigenvalues). The first bifurcation occurs at the point of inflection of the hydrogen peroxide concentration-time curve. This is shown in Figure 3 and Figure 4 as the first vertical line crossing the time axis at $t = 0.9500$ ms. This is not surprising, as hydrogen peroxide serves as the degenerate branching agent for the system. The two dominant explosive modes couple together to form an explosive, oscillating mode (the dominant modes couple together to form a complex conjugate pair, with a positive real part). This marks the point on the solution trajectory where the meta-stable

hydrogen peroxide begins to thermally decompose to hydroxyl radicals, thereby branching, and accelerating exothermic oxidation (thermal runaway).

The second qualitative change in the trajectory occurs when the hydrogen peroxide concentration nears its maximum value. This is shown in Figure 3 and Figure 4 as the dotted line crossing the time axis at $t = 0.9730$ ms. At this point, the dominant eigen-modes change from coupled, explosive, oscillating modes, to coupled, decaying (evanescent), oscillating modes (the real part changes from positive to negative). This marks the point where the rate of thermal decomposition of hydrogen peroxide to hydroxyl radicals is greater than the rate of formation, and the beginning of the thermal explosion of the methanol-air mixture.

The third bifurcation occurs at approximately 2,000 K, when the dominant decaying, oscillating modes disappear, to be replaced by real, evanescent eigen-modes. This is shown in Figure 3 and Figure 4 as the solid vertical line crossing the time axis at $t = 0.9849$ ms. The dominant stable focus describing methanol and formaldehyde oxidation to carbon monoxide is replaced with two real eigen-modes describing the oxidation of carbon monoxide to carbon dioxide, and the reverse reaction.

Appendix 1 shows the eigenvectors that dominate the solution trajectory from the beginning of the auto-ignition process at approximately 1,000 K, through to the chemical equilibrium formed at the adiabatic flame temperature of approximately 2,600K.

Figure 5 shows the magnitude of the rate of formation associated with the dominant eigen-modes as a function of temperature through the auto-ignition from initiation to equilibrium. At the low temperature initiation of auto-ignition, the real eigen-mode describing methanol oxidation dominates the solution trajectory (eigenvector 1), accompanied by its reverse reaction (eigenvector 2). As the

temperature rises, so does the concentration of carbon monoxide. This rise is accompanied by a growing carbon monoxide oxidation reaction to carbon dioxide (eigenvector 3). As the temperature reaches 2,000 K, the methanol and formaldehyde burn out, causing a collapse of the dominant eigen-mode. Wet carbon monoxide oxidation to carbon dioxide suddenly dominates the auto-ignition path to equilibrium, accompanied by its reverse reaction.

(Please insert Figure 5 here.)

Figure 6 shows the evolution of the eigenvalues of the dominant, coupled complex eigen-modes displayed in the complex plane as a function of temperature up to 1,900 K. As the temperature rises above 1,900 K, the methanol and formaldehyde burns out, causing the dominant eigen-modes to collapse, to be replaced with the real, evanescent eigen-modes describing wet CO oxidation to CO₂, and the reverse reaction describing CO₂ reduction back to CO.

The grey curve shown in Figure 6 in the range of temperatures $1,000 \text{ K} < T < 1,165 \text{ K}$ represents the positive real part of the dominant eigenmode eigenvalue. The kink in the grey curve at $T \sim 1,060 \text{ K}$ is associated with the coupling of two real modes to form a complex conjugate pair. The dotted curve shown in Figure 6 represents the imaginary part of the eigenvalue, which is the oscillation frequency of the dominant, coupled modes. At $T \sim 1,165 \text{ K}$, the positive real part changes to a negative real part, which is identified by the solid black curve in Figure 6. The real part of the time constant associated the dominant eigen-mode eigenvalue decreases to $4 \mu\text{s}$ at 1,300 K, down to $1 \mu\text{s}$ at 1,900 K.

Figure 7 shows the real, negative eigenvalues for the other dominant eigenmodes, including that associated with wet CO oxidation to CO₂, and the reverse reduction reaction. The eigenvalue corresponding to the eigenmode representing CO oxidation can be observed to decrease from 1 ms at 1,100 K, down to 0.2 μs at 1,900 K, and then increasing again to approximately 3 μs near equilibrium.

(Please insert Figure 6 here.)

(Please insert Figure 7 here.)

5.2.1 1,000 K < T < 1,090K

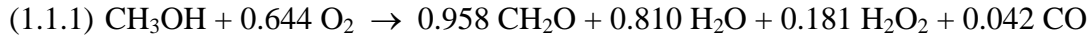
5.2.1.1. T = 1,008 K, P = 36.09 bar

At this temperature and pressure, the solution is dominated by four real eigenmodes (> 95 % of formation and consumption of major species). An approximate local solution for the n'th element of $\mathbf{x}(p, T, t)$ can be expressed as

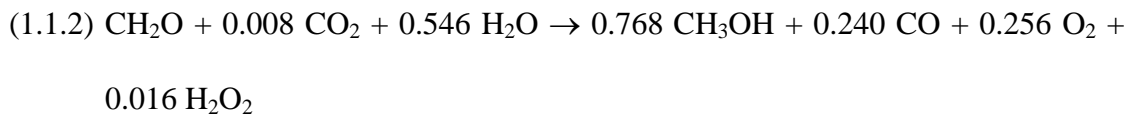
$$x_n(p, T, t) \approx \left(e^{\gamma_1(t-t_0)} - 1\right) \frac{c_1 \lambda_{1n}}{\gamma_1} + \left(e^{\gamma_2(t-t_0)} - 1\right) \frac{c_2 \lambda_{2n}}{\gamma_2} + \left(e^{\gamma_3(t-t_0)} - 1\right) \frac{c_3 \lambda_{3n}}{\gamma_3} + \left(e^{\gamma_4(t-t_0)} - 1\right) \frac{c_4 \lambda_{4n}}{\gamma_4}$$

for the four real, independent modes. The $x_n(t)$ are the elements of the vector $\mathbf{x}(p, T, t)$, while λ_{mn} refers to the n vector elements of the m 'th eigenvector. γ_m refers to the m 'th eigenvalue, and c_m refers to the rate of production of species for the m 'th eigen-mode.

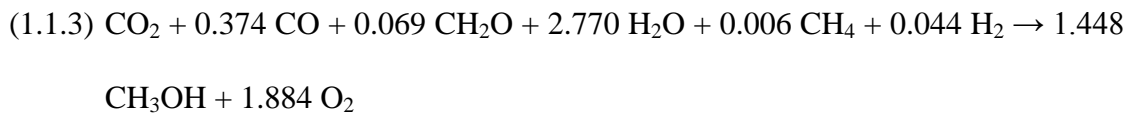
The approximate solution for the eigen-mode rates $\mathbf{c}(p, T, t)$ are obtained from the eigenvectors presented in Appendix 1, and can be expressed in reaction form, which is described by



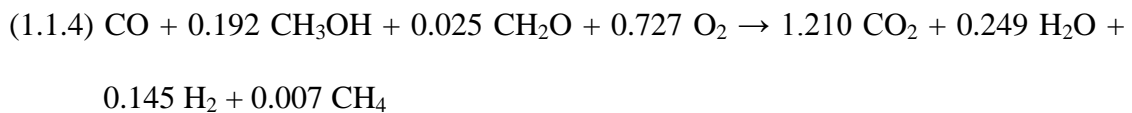
$$\gamma_1 = 5029 \text{ s}^{-1}, c_1 = 1499 \text{ mole.m}^{-3}.\text{s}^{-1}$$



$$\gamma_2 = -704 \text{ s}^{-1}, c_2 = 441 \text{ mole.m}^{-3}.\text{s}^{-1}$$



$$\gamma_3 = 8.2 \text{ s}^{-1}, c_3 = 122.0 \text{ mole.m}^{-3}.\text{s}^{-1}$$

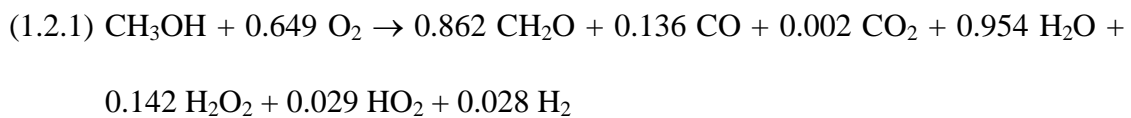


$$\gamma_4 = -18.1 \text{ s}^{-1}, c_4 = 148.6 \text{ mole.m}^{-3}.\text{s}^{-1}$$

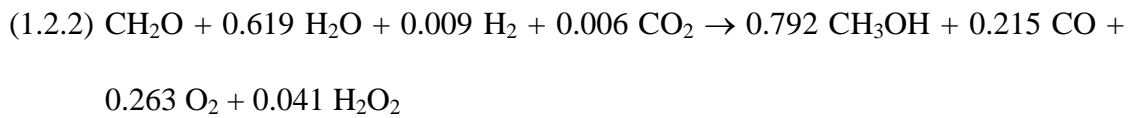
The dominant mode (reaction 1.1.1) is an explosive mode with a reaction time-scale of 0.20 ms, involving the exothermic oxidation of methanol to form formaldehyde, water, and the degenerate branching agent hydrogen peroxide. The second important eigen-mode (reaction 1.1.2) describes an endothermic reverse reaction between formaldehyde and water, to form methanol, oxygen, and importantly, more hydrogen peroxide.

5.2.1.2 T = 1,028 K, P = 39.16 bar

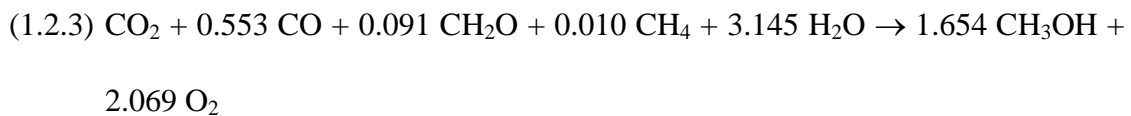
At this temperature and pressure, the four dominant modes remain (> 95% of formation and consumption of major species). The first, and most important, is just an evolution of the dominant explosive mode from above. The second dominant mode combines the reverse reaction with formaldehyde oxidation to CO. The third mode describes an endothermic reverse reaction of CO₂, CO and formaldehyde to methanol. The fourth mode describes the exothermic oxidation of carbon monoxide to carbon dioxide.



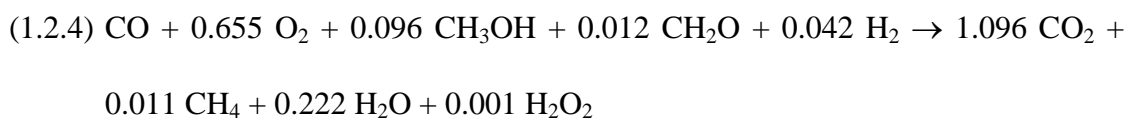
$$\gamma_1 = 5\,561 \text{ s}^{-1}, c_1 = 6\,918 \text{ mole}\cdot\text{m}^{-3}\cdot\text{s}^{-1}$$



$$\gamma_2 = -2\,474 \text{ s}^{-1}, c_2 = 925.0 \text{ mole}\cdot\text{m}^{-3}\cdot\text{s}^{-1}$$



$$\gamma_3 = 41.1 \text{ s}^{-1}, c_3 = 587.7 \text{ mole}\cdot\text{m}^{-3}\cdot\text{s}^{-1}$$



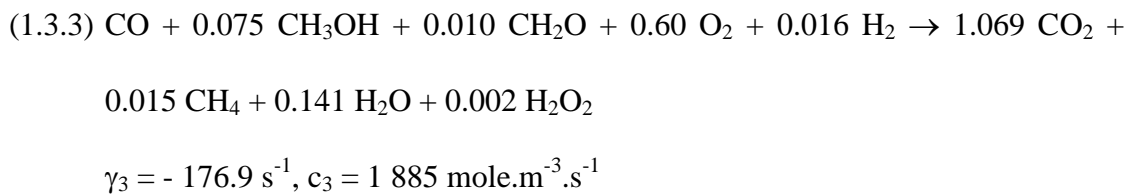
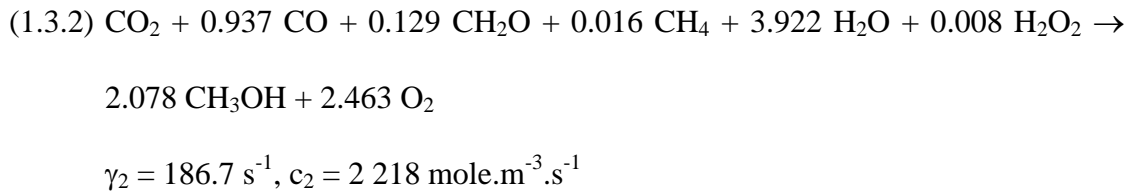
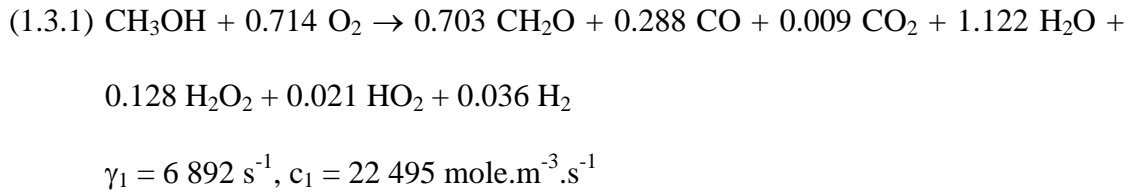
$$\gamma_4 = -67.6 \text{ s}^{-1}, c_4 = 523.6 \text{ mole}\cdot\text{m}^{-3}\cdot\text{s}^{-1}$$

5.2.1.3 T = 1,048 K, P = 41.34 bar

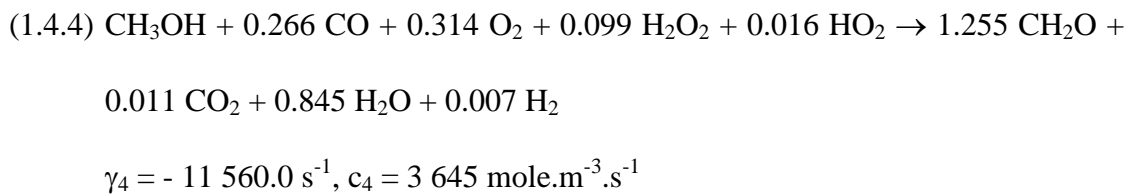
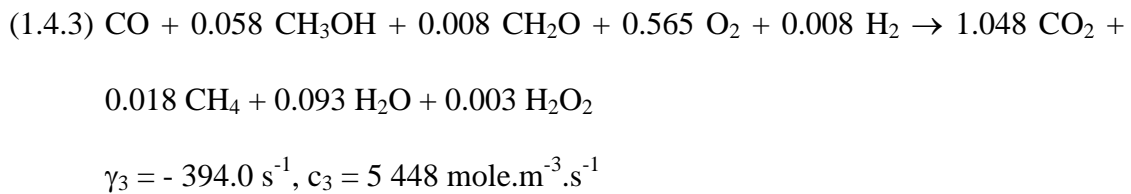
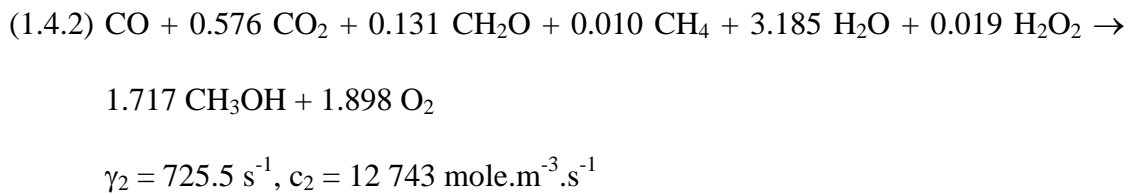
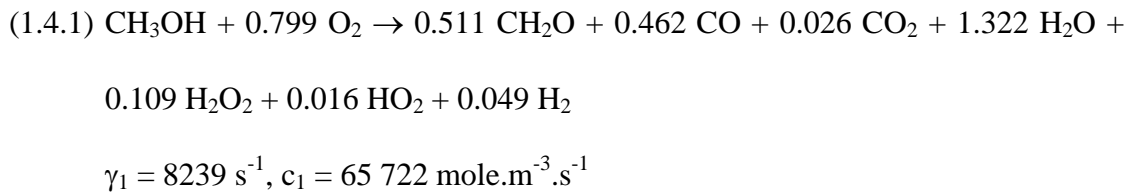
As the temperature of the system reaches 1,048 K, the system is qualitatively described by a three-mode solution, which is of the form

$$x_n(p, T, t) \approx \left(e^{\gamma_1(t-t_0)} - 1\right) \frac{c_1 \lambda_{1n}}{\gamma_1} + \left(e^{\gamma_2(t-t_0)} - 1\right) \frac{c_2 \lambda_{2n}}{\gamma_2} + \left(e^{\gamma_3(t-t_0)} - 1\right) \frac{c_3 \lambda_{3n}}{\gamma_3}$$

for three real, independent eigen-modes. Qualitatively, the system is three-dimensional in nature, dominated by the first mode discussed above. The locus of regular points in this part of the trajectory of the system is a locus of explosive, real modes. The eigen-mode rates of formation and consumption are expressed in reaction form.

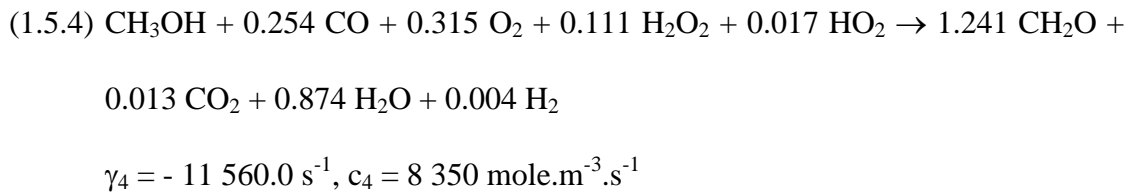
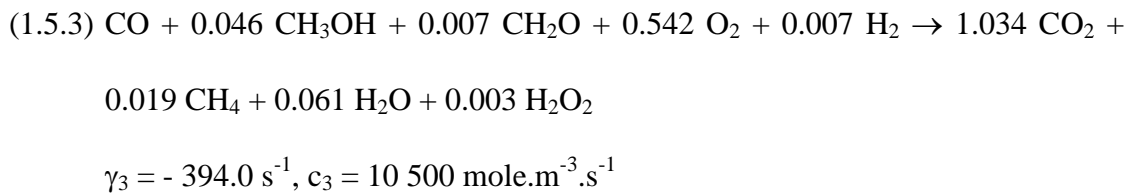
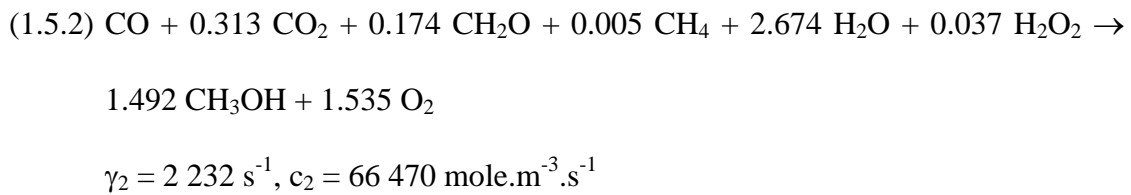
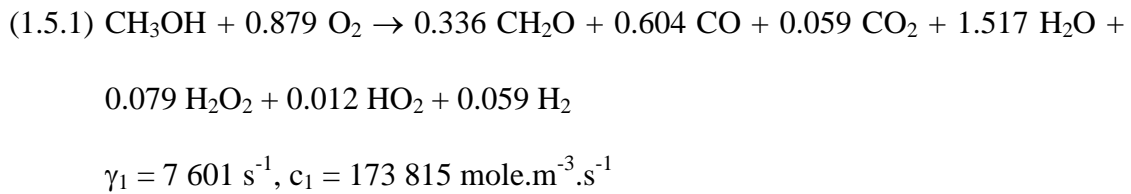


5.2.1.4. T = 1,071 K, P = 42.70 bar



As the temperature of the combustion system reaches 1,088 K, the two competing exponentially increasing modes that dominate the qualitative behaviour of the system in this temperature regime are of similar importance, since the rates of production of species from the two dominant modes are of opposite sign, and approximately equal magnitude.

5.2.1.5. T = 1,088 K, P = 43.26 bar



5.2.2. 1,090 K < T < 1,170 K, 43.4 bar < P < 44.1 bar

In this temperature regime the two explosive modes that previously dominated the auto-ignition trajectory couple together to form a complex conjugate pair with a positive real part, defining a decaying, oscillating mode.

The evolving coupled modes are related to the onset of hydrogen peroxide decomposition to hydroxyl radicals, and the consequent increase in methanol

oxidation. These reactions are exothermic, and the heat liberated is now sufficient to heat the end-gas methanol/air mixture.

The change in the chemistry is reflected by the bifurcation in the trajectory of the system, and, as pointed out earlier, occurs at the point of inflection of the hydrogen peroxide concentration trajectory in time. In other words, the change in the structure of the chemical rate equations occurs when the second time derivative of the hydrogen peroxide concentration is zero. The point in time when the bifurcation occurs is shown in Figures 2 and 3 by the first vertical line along the time axis, occurring at time $t = 0.9500$ ms.

The rate of reaction associated with the explosive, oscillating mode is approximately nine times larger than that of the next largest mode. Therefore, these two coupled modes dominate the linear solution space of the chemical system. If the eigenvalues of the coupled, exponentially increasing, oscillatory modes are $\gamma + i\omega$ and $\gamma - i\omega$ respectively, the coupled two mode solution vector has the form

$$x_n(t) \approx a_1(t)\lambda_{1n} + a_2(t)\lambda_{2n} = [e^{(\gamma+i\omega)t} - 1] \frac{(c_r + ic_i)(\lambda_{rn} + i\lambda_{in})}{(\gamma + i\omega)} + [e^{(\gamma-i\omega)t} - 1] \frac{(c_r - ic_i)(\lambda_{rn} - i\lambda_{in})}{(\gamma - i\omega)}$$

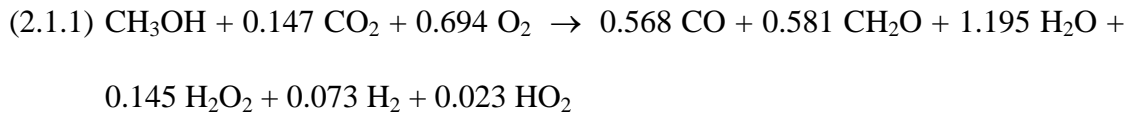
where λ_{rn} and λ_{in} are the real and imaginary elements of the eigenvector λ , c_r and c_i are the time independent real and imaginary components of the projection of the normalised eigenvector λ onto the vector describing the rate of species production dx/dt . This approximate solution for the elements of x can be re-expressed in the form

$$x_n(t) \approx \frac{2(e^{\gamma t} \cos \omega t - 1)[\lambda_{rn}(c_r \gamma + c_i \omega) - \lambda_{in}(c_i \gamma - c_r \omega)]}{\gamma^2 + \omega^2} - \frac{2e^{\gamma t} \sin \omega t [\lambda_{in}(c_r \gamma + c_i \omega) + \lambda_{rn}(c_i \gamma - c_r \omega)]}{\gamma^2 + \omega^2}$$

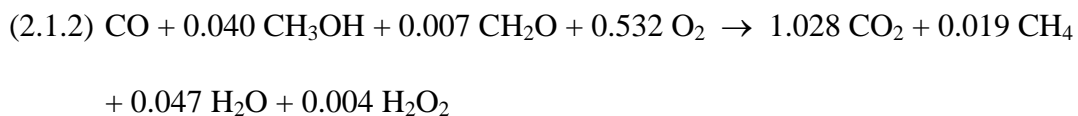
The elements of \mathbf{x} ($x_n(t)$) increase exponentially with a time dependence given by the real part of γ , and simultaneously oscillates with frequency ω .

Examining the evolution of the complex eigenvalues reveals that the rate of exponential increase decreases with time, and the frequency of oscillation increases relative to the rate of exponential increase. The time scales defined by the dominant complex eigenvalues and the evolution of the chemistry result in there not being enough time for the system to pass through a single oscillation before a second qualitative transition takes place. Chemically, this means that the net rate of production of degenerate branching agent (hydrogen peroxide) in the methanol/air oxidation system begins to decrease.

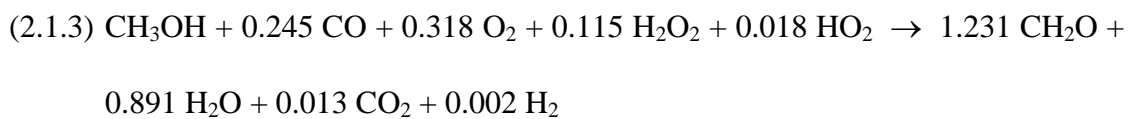
5.2.2.1. T = 1,097 K, P = 43.45 bar



$$\gamma_1 = 5\,053 + 1439i \text{ s}^{-1}, |c_1| = 95\,000 \text{ mole.m}^{-3}.\text{s}^{-1}$$

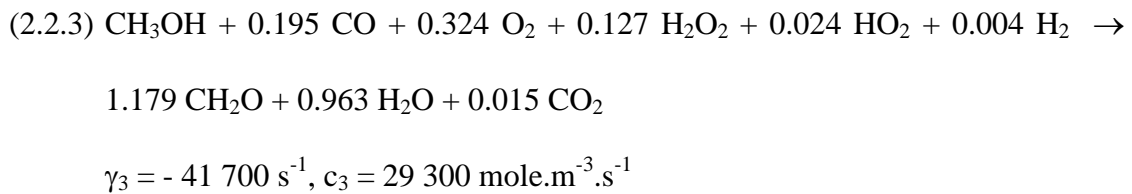
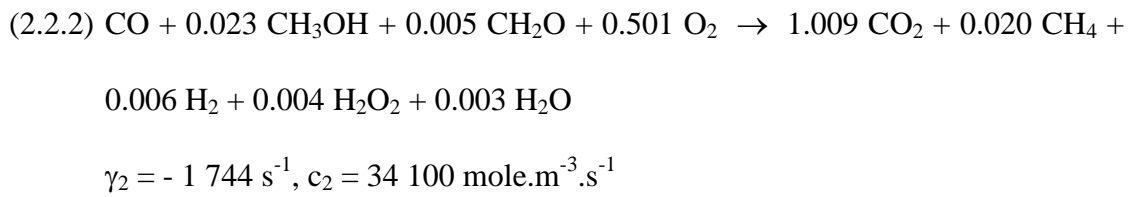
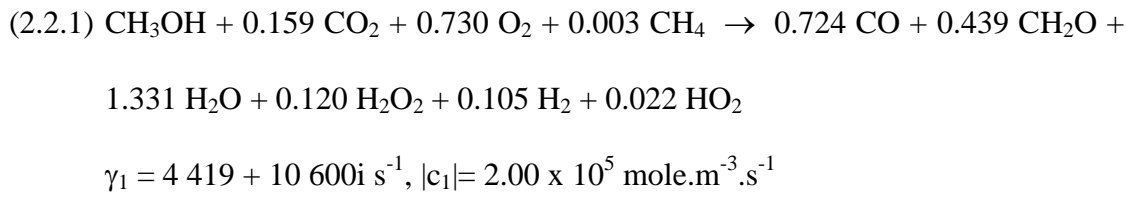


$$\gamma_2 = -828.8 \text{ s}^{-1}, c_2 = 14\,100 \text{ mole.m}^{-3}.\text{s}^{-1}$$

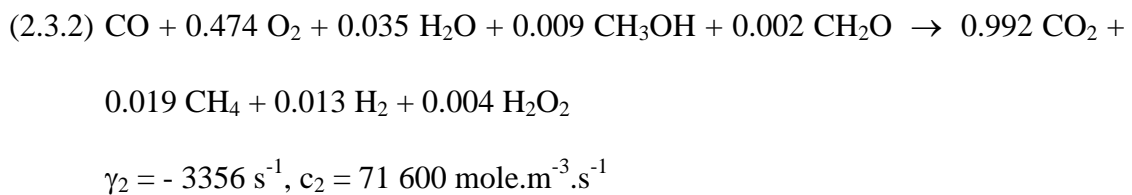
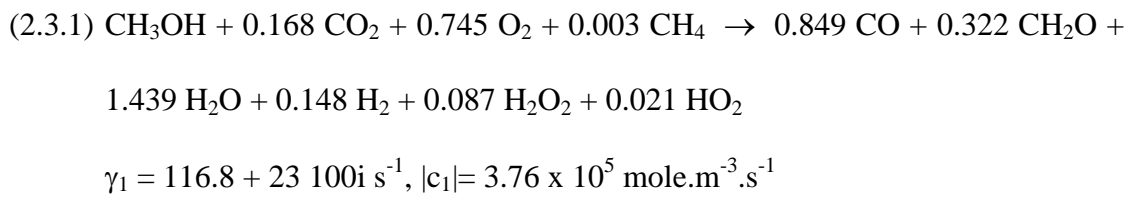


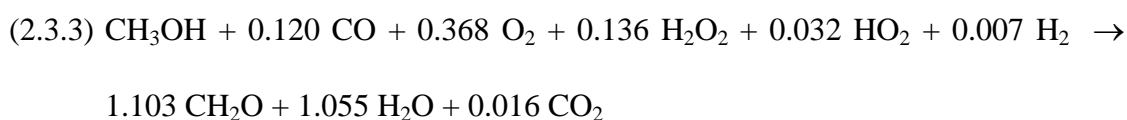
$$\gamma_3 = -21\,710 \text{ s}^{-1}, c_3 = 11\,600 \text{ mole.m}^{-3}.\text{s}^{-1}$$

5.2.2.2. T = 1,130 K, P = 43.85 bar



5.2.2.3. T = 1,165 K, P = 44.04 bar





$$\gamma_3 = -76\,350 \text{ s}^{-1}, c_3 = 62\,700 \text{ mole}\cdot\text{m}^{-3}\cdot\text{s}^{-1}$$

Reactions 2.3.1 and 2.3.2 are quasi-termination reactions in that they both produce degenerate branching agent hydrogen peroxide. The reaction system is also self-heating through the exothermic production of CH₂O, H₂O, CO, and CO₂.

5.2.3. 1,170 K < T < 2,000 K, 44.1 bar < P < 44.6 bar

Thermal runaway begins at this stage of auto-ignition. Mathematically, the dominant eigen-mode undergoes a pseudo-bifurcation from an unstable focus to a stable focus. This change is a consequence of the coupled exponentially increasing, oscillatory modes changing to coupled, exponentially decaying, oscillatory modes. This means that the chemical system will now converge towards its equilibrium point, along an inward spiral. As this transition takes place, other real evanescent modes are introduced that are also important in the evolution of the system.

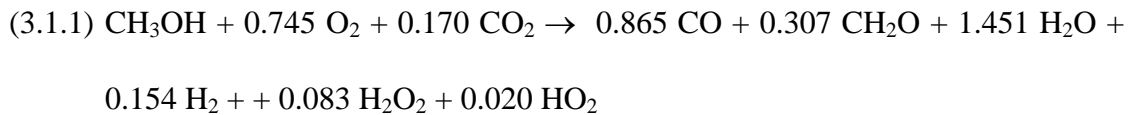
The pseudo-bifurcation from an explosive, oscillating mode to a decaying, oscillating mode of the dominant eigen-mode occurs when hydrogen peroxide nears its maximum concentration. In other words, the pseudo-bifurcation occurs in a neighbourhood of the point when the first time derivative of the hydrogen peroxide concentration is zero. This is shown by the second vertical line along the time axis in Figures 2 and 3. This point can be used to define the beginning of thermal runaway.

Chemically, the system is now described in terms of a branching reaction sequence. The intermediate chemical species (apart from hydrogen peroxide) quickly

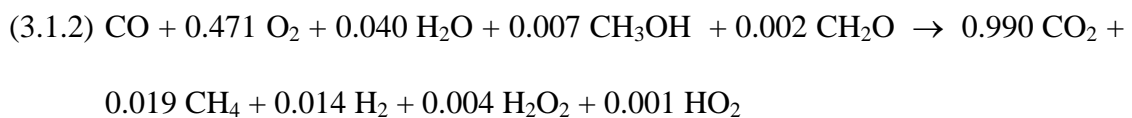
reach their maximum concentrations, simultaneous with thermal explosion, through the rapid oxidation of methanol by hydroxyl radicals and molecular oxygen to formaldehyde and water, followed by the oxidation of formaldehyde to carbon monoxide. The rapid release of heat into the gas mixture causes the temperature of the gas to rise far more rapidly than the rate of increase of the external pressure. Consequently, the gas expands rapidly, and the species concentrations decrease.

The exponentially decaying oscillatory modes reflect the chemically explosive condition of the methanol/air oxidation system as explained earlier. The dominant coupled complex eigen-modes explain the exothermic chemistry in terms of the oxidation reactions of methanol to formaldehyde and water, followed by the oxidation reactions of formaldehyde to carbon monoxide and water. The dominance of these two coupled modes continues to about 2000 K, at which time the mode reflecting the wet oxidation of carbon monoxide to carbon dioxide begins to take over, and dominates the system in the thermally explosive regime 2,000 K to equilibrium at approximately 2,600 K.

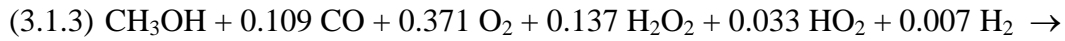
5.2.3.1 T = 1,169 K, P = 44.06 bar



$$\gamma_1 = -969.1 + 25\,000i \text{ s}^{-1}, |c_1| = 4.02 \times 10^5 \text{ mole.m}^{-3}.\text{s}^{-1}$$



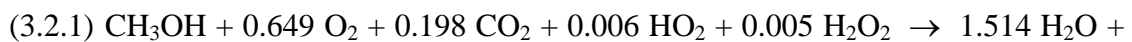
$$\gamma_2 = -3\,617 \text{ s}^{-1}, c_2 = 77\,900 \text{ mole.m}^{-3}.\text{s}^{-1}$$



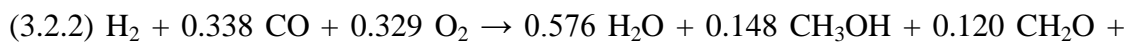
$$\gamma_3 = -82\,010 \text{ s}^{-1}, c_3 = 67\,700 \text{ mole.m}^{-3}.\text{s}^{-1}$$

Reaction 3.1.1 which evolves into reaction 3.2.1 below shows the transition of the auto-ignition system through the net formation of degenerate branching agent hydrogen peroxide (reaction 3.1.1) to the net consumption of hydrogen peroxide (reaction 3.2.1).

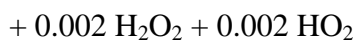
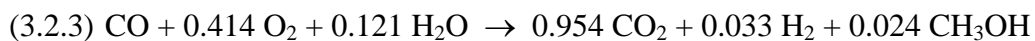
5.2.3.2 T = 1,294 K, P = 44.25 bar



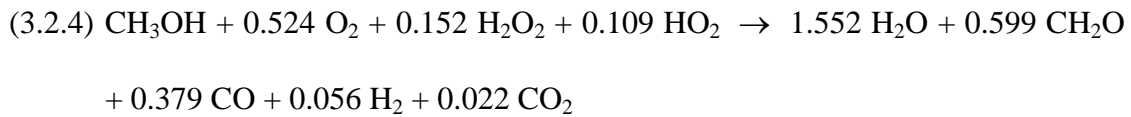
$$\gamma_1 = -104\,100 + 96\,560i \text{ s}^{-1}, |c_1| = 1.608 \times 10^6 \text{ mole.m}^{-3}.\text{s}^{-1}$$



$$\gamma_2 = -78\,270 \text{ s}^{-1}, c_2 = 4.99 \times 10^5 \text{ mole.m}^{-3}.\text{s}^{-1}$$



$$\gamma_3 = -18\,490 \text{ s}^{-1}, c_3 = 4.26 \times 10^5 \text{ mole.m}^{-3}.\text{s}^{-1}$$

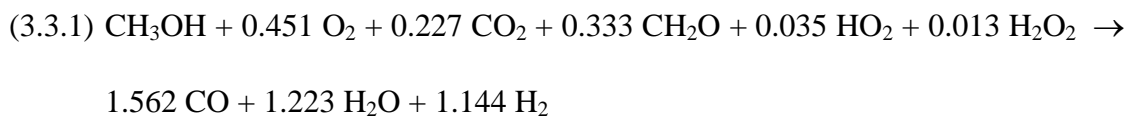


$$\gamma_4 = -484\,800 \text{ s}^{-1}, c_4 = 4.45 \times 10^5 \text{ mole.m}^{-3}.\text{s}^{-1}$$

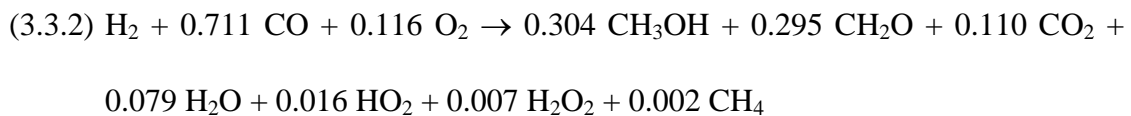
Reactions 3.2.1 above and 3.3.1 below mark the temperature regime (1,300 K < T < 1,400 K) where the formaldehyde concentration reaches its maximum value. For larger temperatures (T > 1,400K), formaldehyde is oxidized to carbon monoxide and water.

Reactions 3.2.2 above and 3.3.2 below contain the reverse reaction to Reactions 3.2.1 and 3.3.1, growing in magnitude with temperature. Reactions 3.2.3 above and 3.3.3 below are the reactions describing the exothermic oxidation of carbon monoxide to carbon dioxide.

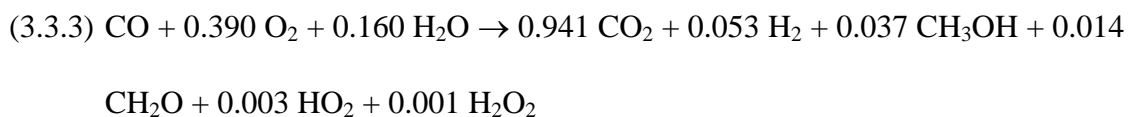
5.2.3.3. T = 1,406 K, P = 44.30 bar



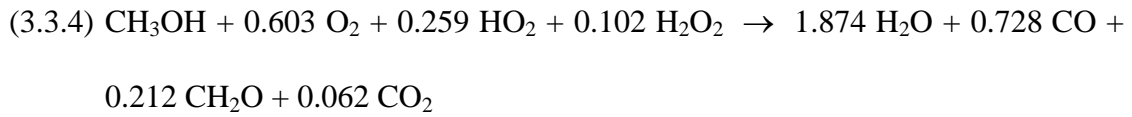
$$\gamma_1 = -2.468 \times 10^5 + 1.190 \times 10^5 i \text{ s}^{-1}, |c_1| = 3.38 \times 10^6 \text{ mole.m}^{-3}.\text{s}^{-1}.$$



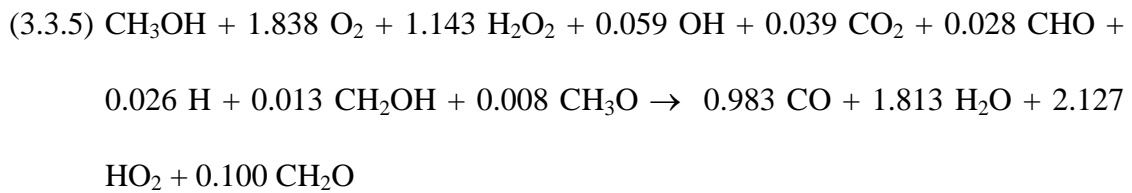
$$\gamma_2 = -1.879 \times 10^5 \text{ s}^{-1}, c_2 = 3.26 \times 10^6 \text{ mole.m}^{-3}.\text{s}^{-1}$$



$$\gamma_3 = -39\,640 \text{ s}^{-1}, c_3 = 8.24 \times 10^5 \text{ mole.m}^{-3}.\text{s}^{-1}$$

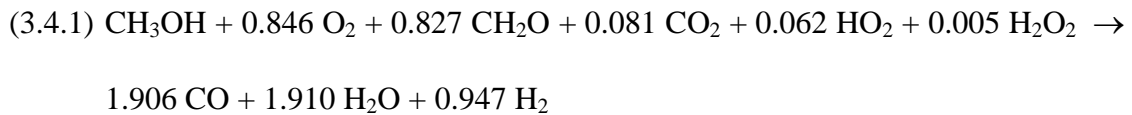


$$\gamma_4 = 1.405 \times 10^6 \text{ s}^{-1}, c_4 = 5.85 \times 10^5 \text{ mole.m}^{-3}.\text{s}^{-1}$$

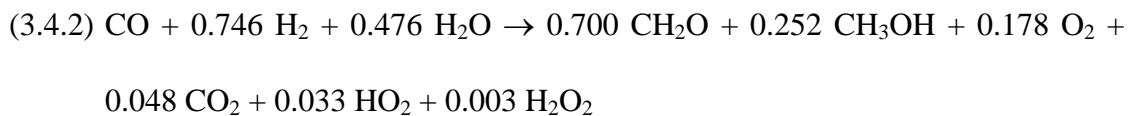


$$\gamma_5 = -1.239 \times 10^8 \text{ s}^{-1}, c_5 = 99\,008 \text{ mole.m}^{-3}.\text{s}^{-1}$$

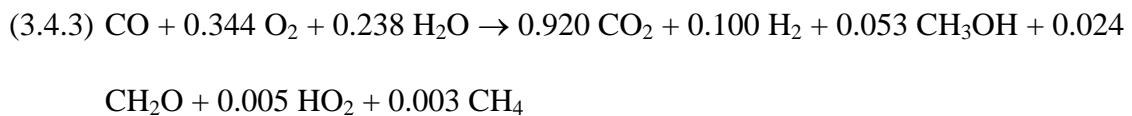
5.2.3.4. T = 1,548 K, P = 44.34 bar



$$\gamma_1 = -3.062 \times 10^5 + 2.089 \times 10^5 i \text{ s}^{-1}, |c_1| = 4.62 \times 10^6 \text{ mole.m}^{-3}.\text{s}^{-1}$$

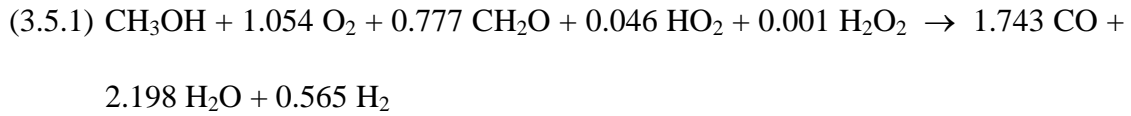


$$\gamma_2 = -5.706 \times 10^5 \text{ s}^{-1}, c_2 = 4.26 \times 10^6 \text{ mole.m}^{-3}.\text{s}^{-1}$$

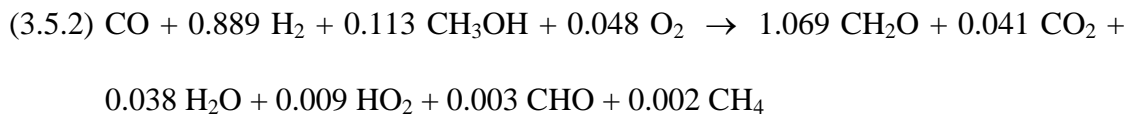


$$\gamma_3 = -64\,740 \text{ s}^{-1}, c_3 = 1.12 \times 10^6 \text{ mole.m}^{-3}.\text{s}^{-1}$$

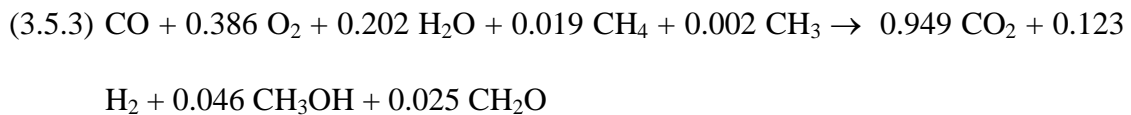
5.2.3.5 T= 1,689 K, P = 44.36 bar



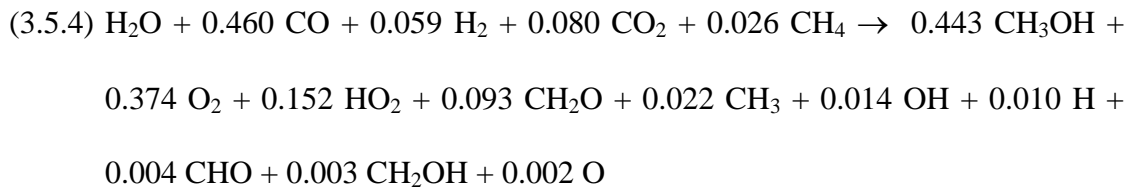
$$\gamma_1 = -4.904 \times 10^5 + 7.411 \times 10^5 i \text{ s}^{-1}, |c_1| = 6.168 \times 10^6 \text{ mole.m}^{-3} \cdot \text{s}^{-1}$$



$$\gamma_2 = -1.998 \times 10^6 \text{ s}^{-1}, c_2 = 1.770 \times 10^6 \text{ mole.m}^{-3} \cdot \text{s}^{-1}$$

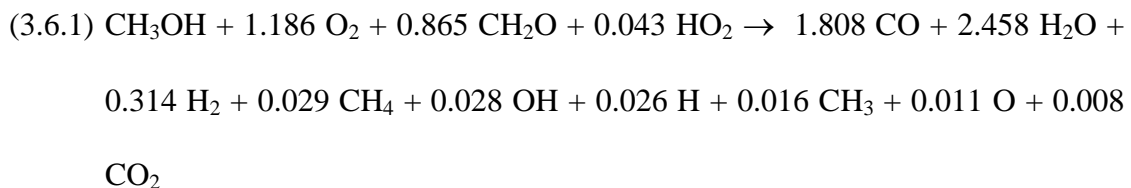


$$\gamma_3 = -1.067 \times 10^5 + 1.074 \times 10^5 i \text{ s}^{-1}, |c_3| = 1.642 \times 10^6 \text{ mole.m}^{-3} \cdot \text{s}^{-1}$$

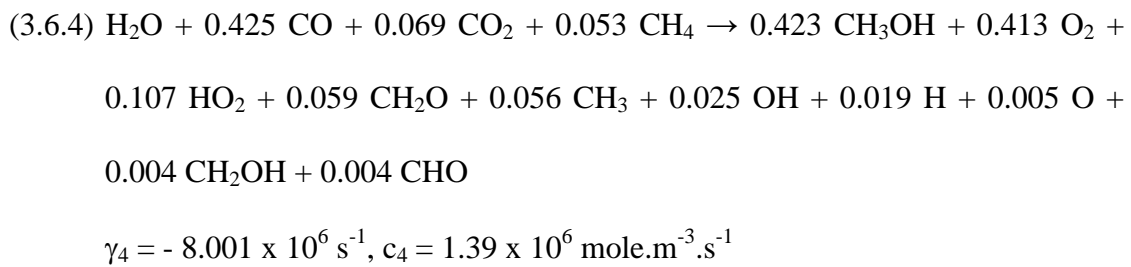
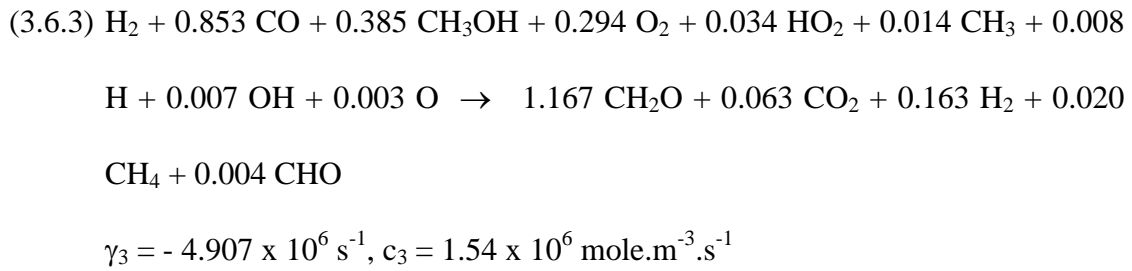
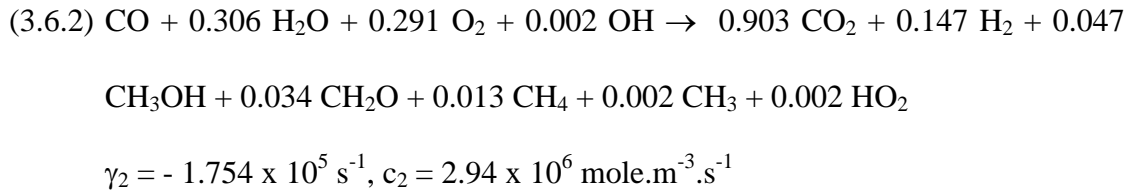


$$\gamma_4 = -5.151 \times 10^6 \text{ s}^{-1}, c_4 = 1.03 \times 10^6 \text{ mole.m}^{-3} \cdot \text{s}^{-1}$$

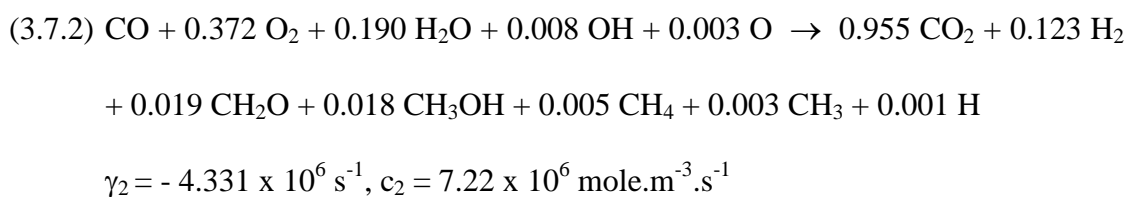
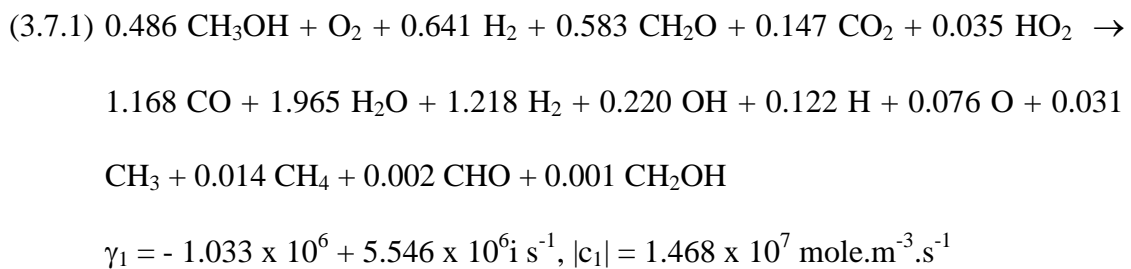
5.2.3.6. T = 1,774 K, P = 44.37 bar

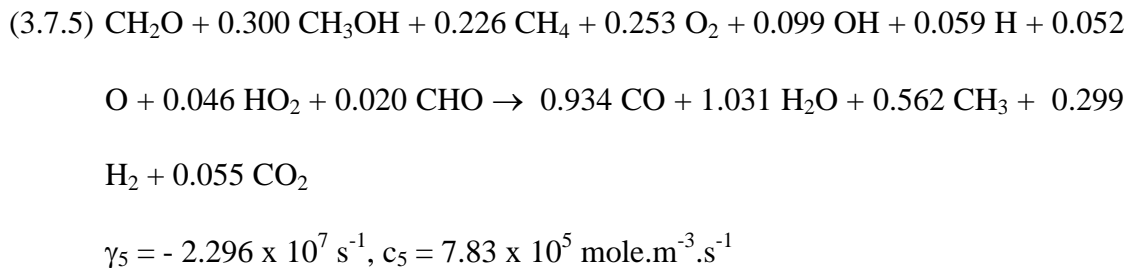
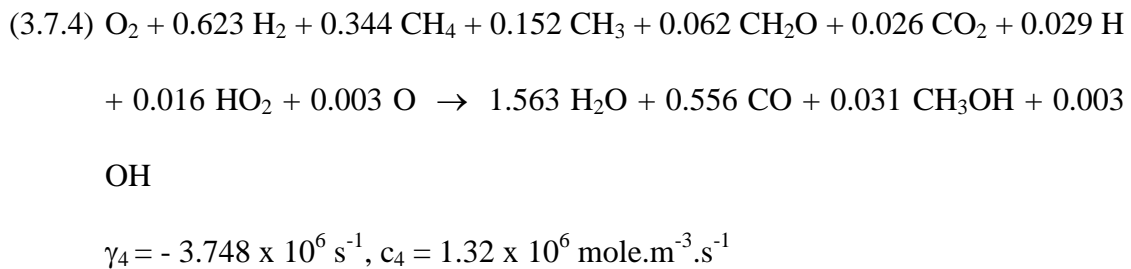
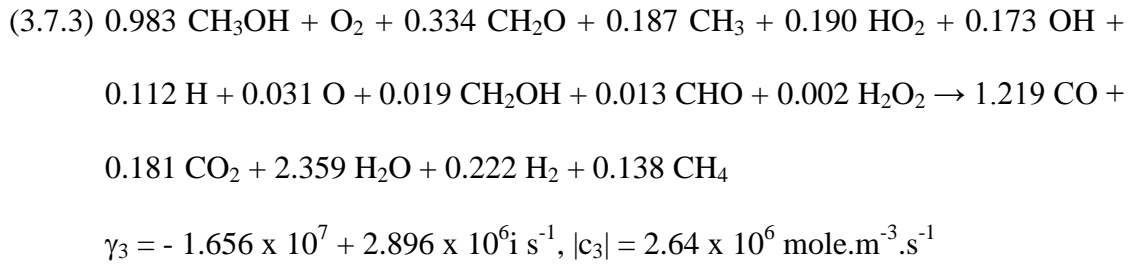


$$\gamma_1 = -7.371 \times 10^5 + 1.896 \times 10^6 i \text{ s}^{-1}, |c_1| = 8.683 \times 10^6 \text{ mole.m}^{-3} \cdot \text{s}^{-1}$$



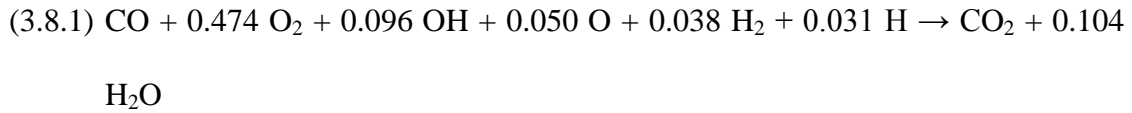
5.2.3.7 T = 1,900 K, P = 44.37 bar



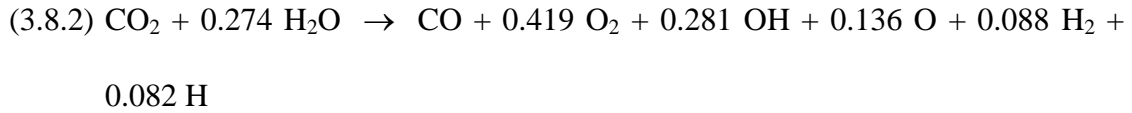


5.2.3.8 T = 2,096 K, P = 44.38 bar

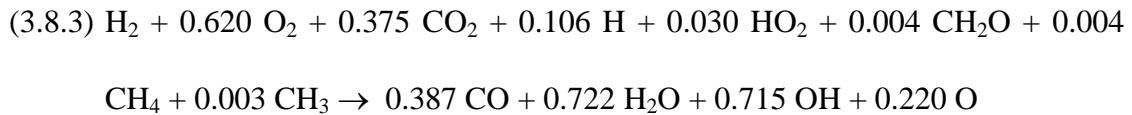
In the temperature range of $1,900 < T < 2,100$, the previously dominant, coupled, complex eigen-modes describing the oxidation of methanol and formaldehyde to carbon monoxide and water disappears, to be replaced with real, evanescent eigen-modes describing the wet oxidation of carbon monoxide to carbon dioxide and water, and the reverse reaction. The solution trajectory of the auto-ignition system approaches equilibrium along stable proper nodes.



$$\gamma_1 = - 2.343 \times 10^6 \text{ s}^{-1}, c_1 = 3.21 \times 10^7 \text{ mole.m}^{-3}.\text{s}^{-1}$$

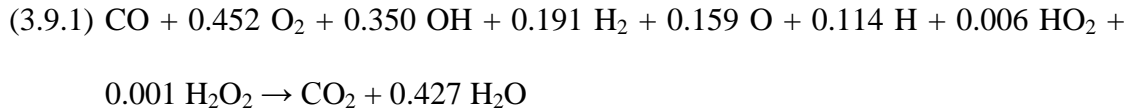


$$\gamma_2 = - 4.395 \times 10^6 \text{ s}^{-1}, c_2 = 1.35 \times 10^7 \text{ mole.m}^{-3}.\text{s}^{-1}$$

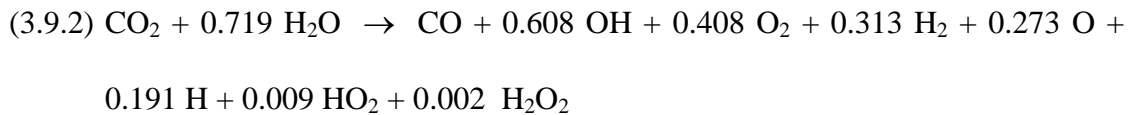


$$\gamma_3 = - 2.309 \times 10^7 \text{ s}^{-1}, c_3 = 1.78 \times 10^6 \text{ mole.m}^{-3}.\text{s}^{-1}$$

5.2.3.9 T = 2,314 K, P = 44.39 bar



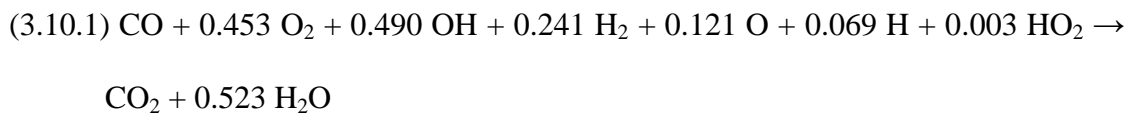
$$\gamma_1 = - 2.880 \times 10^6 \text{ s}^{-1}, c_1 = 2.25 \times 10^7 \text{ mole.m}^{-3}.\text{s}^{-1}$$



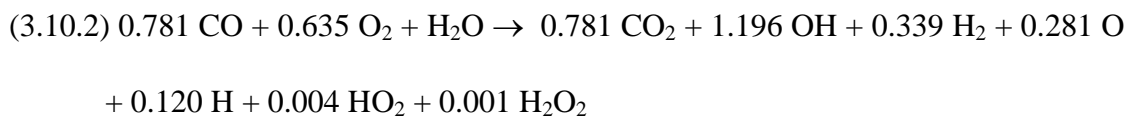
$$\gamma_2 = - 3.664 \times 10^6 \text{ s}^{-1}, c_2 = 1.33 \times 10^7 \text{ mole.m}^{-3}.\text{s}^{-1}$$

5.2.3.10 T = 2,519 K, P = 44.46 bar

As the solution trajectory approaches equilibrium along stable nodes (real, evanescent eigen-modes), the dominant reaction rates decrease rapidly, and the molecular species present begin to equilibrate.

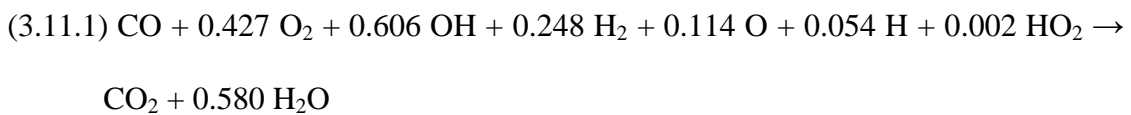


$$\gamma_1 = - 5.829 \times 10^5 \text{ s}^{-1}, c_1 = 3.33 \times 10^5 \text{ mole.m}^{-3}.\text{s}^{-1}$$

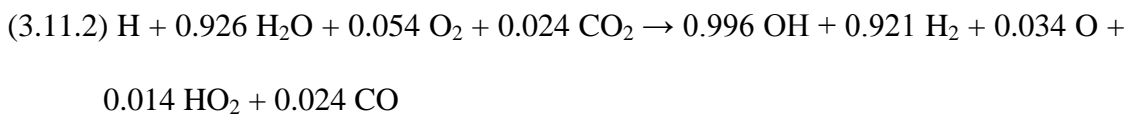


$$\gamma_2 = - 2.808 \times 10^6 \text{ s}^{-1}, c_2 = 1.96 \times 10^4 \text{ mole.m}^{-3}.\text{s}^{-1}$$

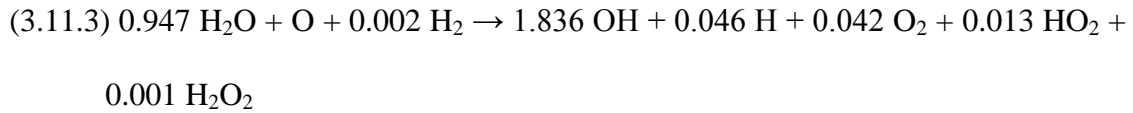
5.2.3.11 T = 2,553 K, P = 44.63 bar



$$\gamma_1 = - 3.094 \times 10^5 \text{ s}^{-1}, c_1 = 1.43 \times 10^4 \text{ mole.m}^{-3}.\text{s}^{-1}$$



$$\gamma_2 = - 1.015 \times 10^9 \text{ s}^{-1}, c_2 = 1.16 \times 10^4 \text{ mole.m}^{-3}.\text{s}^{-1}$$



$$\gamma_3 = -2.204 \times 10^8 \text{ s}^{-1}, c_3 = 7\,380 \text{ mole.m}^{-3}.\text{s}^{-1}$$



$$\gamma_4 = -6.396 \times 10^9 \text{ s}^{-1}, c_4 = 3270 \text{ mole.m}^{-3}.\text{s}^{-1}$$

The auto-ignition reactions and combustion product species reach equilibrium at approximately 2,550 K – 2,600 K. The rates for formation associated with the dominant eigen-modes decrease exponentially to small values, effectively freezing the equilibrium state.

6. Summary and Conclusion

The eigen-mode analysis presented here provided a direct method of determining the dominant reaction modes, the critical points in the evolution of the system, and the means to determine the nature of the locus of regular points constituting the solution trajectory of the system from the initial state to chemical equilibrium.

The sudden changes in the analytic structure of the dominant eigen-modes defined the changes that occurred in the solution trajectory in the generalized phase space of the auto-ignition system. These were determined in the low temperature regime ($1,100 \text{ K} < T < 1,200 \text{ K}$) by the critical points in the evolution trajectory of the degenerate branching agent, hydrogen peroxide. For temperatures $T < 1,090 \text{ K}$, the dominant eigen-modes had eigenvalues that were real and positive. At $T = 1,090 \text{ K}$,

the forward reaction describing methanol oxidation to formaldehyde, carbon monoxide and water and the reverse reaction coupled together, causing a qualitative change in the reaction rates. This qualitative change occurred at the point of inflection of the hydrogen peroxide concentration trajectory, and was identified by the eigenvalues changing from positive real numbers to complex conjugate pairs. The dominant explosive modes coupled to form an explosive, oscillating mode.

As the temperature increased towards 1,168 K, the real part of the dominant, coupled complex eigenvalues changed sign from positive to negative. The change in sign at $T = 1,068$ K caused the dominant explosive, oscillating mode to change to a decaying, oscillating mode. This change was observed to occur in the neighbourhood of the maximum of the hydrogen peroxide concentration trajectory. These results are important, for they relate the mathematical structure of the solution of the chemical rate equations directly to the evolution of the concentration of the degenerate branching agent.

The qualitative change at high temperature ($T \sim 2,000$ K) occurred when the methanol and formaldehyde oxidation to carbon monoxide was replaced by wet carbon monoxide oxidation to carbon dioxide. The dominant coupled complex modes describing a decaying, oscillating mode disappeared, to be replaced with two stable nodes with real, negative eigenvalues. These stable nodes described wet carbon monoxide oxidation to carbon dioxide, and the reverse reduction reaction.

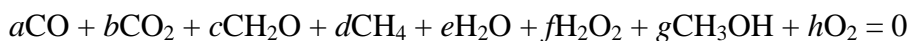
Appendix 1 – Dominant Eigen-modes Describing Methanol-Air Auto-Ignition

Eigenvector 1:



Temperature (K)	γ_1 (/s)	c_1 (mole/m ³ s)	CH ₃ OH	O ₂	CH ₂ O	CO	CO ₂	H ₂ O	H ₂ O ₂	HO ₂	H ₂
1008	5029	1499	-1.000	-0.644	0.958	0.042	0.000	0.810	0.181	0.000	0.000
1028	5561	6918	-1.000	-0.649	0.862	0.136	0.002	0.954	0.142	0.029	0.028
1048	6892	22495	-1.000	-0.714	0.703	0.288	0.009	1.122	0.128	0.021	0.036
1071	8239	65722	-1.000	-0.799	0.511	0.462	0.026	1.322	0.109	0.016	0.049
1088	7601	173815	-1.000	-0.879	0.336	0.604	0.059	1.517	0.079	0.012	0.059

Eigenvector 2:



Temperature (K)	γ_2 (/s)	c_2 (mole/m ³ s)	CH ₃ OH	O ₂	CH ₂ O	CO	CO ₂	CH ₄	H ₂ O	H ₂ O ₂
1008	8.20	122.0	1.448	1.884	-0.069	-0.374	-1.000	-0.006	-2.770	0.000
1028	41.1	587.7	1.654	2.069	-0.091	-0.553	-1.000	-0.010	-3.145	0.000
1048	187	2218	2.078	2.463	-0.129	-0.937	-1.000	-0.016	-3.922	-0.008
1071	726	12743	1.717	1.898	-0.131	-1.000	-0.576	-0.010	-3.185	-0.019
1088	2232	66470	1.492	1.535	-0.174	-1.000	-0.313	-0.005	-2.674	-0.037

Eigenvector 1 + Eigenvector 2:



Temp- erature (K)	γ_1 (/s)	ω_1 (/s)	$ c_i $ <i>mole/m³s</i>	CH ₃ OH	O ₂	CH ₂ O	CO	CO ₂	H ₂ O	H ₂ O ₂	HO ₂	H ₂
1097	5053	1439	95000	-1.000	-0.694	0.581	0.568	-0.147	1.195	0.145	0.023	0.073
1130	4419	10600	2.00x10 ⁵	-1.000	-0.730	0.439	0.724	-0.159	1.331	0.120	0.022	0.105
1165	116.8	23100	3.76x10 ⁵	-1.000	-0.745	0.322	0.849	-0.168	1.439	0.087	0.021	0.148
1169	-969	25000	4.02x10 ⁵	-1.000	-0.745	0.307	0.865	-0.170	1.451	0.083	0.020	0.154
1294	-104100	96560	1.61x10 ⁶	-1.000	-0.649	0.009	1.191	-0.198	1.514	-0.005	-0.006	0.490
1406	-246800	119000	3.38x10 ⁶	-1.000	-0.451	-0.333	1.562	-0.227	1.223	-0.013	-0.035	1.144
1548	-306200	208900	4.62x10 ⁶	-1.000	-0.846	-0.827	1.906	-0.081	1.910	-0.005	-0.062	0.947
1689	-490400	741100	6.17x10 ⁶	-1.000	-1.054	-0.777	1.743	0.000	2.198	-0.001	-0.046	0.565
1774	-737100	1 896000	8.68x10 ⁶	-1.000	-1.186	-0.865	1.808	0.008	2.458	0.000	-0.043	0.314
1900	-1033000	5 546000	7.14x10 ⁶	-1.000	-2.058	-1.200	2.405	-0.303	4.046	0.000	-0.072	-1.320

Eigenvector 3:



Temp- erature (K)	γ_3 (/s)	c_3 <i>mole/m³s</i>	CH ₃ OH	O ₂	CH ₂ O	CO	CO ₂	H ₂ O	H ₂ O ₂	HO ₂	H ₂	CH ₄
1294	-78 270	499 000	0.148	-0.329	0.120	-0.338	0.070	0.576	0.004	0.003	-1.000	0.001
1406	-187900	3.26x10 ⁶	0.304	-0.116	0.295	-0.711	0.110	0.079	0.007	0.016	-1.000	0.002
1548	-570 060	4.26x10 ⁶	0.252	0.178	0.700	-1.000	0.048	-0.476	0.003	0.033	-0.746	0.000
1689	-1998000	1.77x10 ⁶	-0.113	-0.048	1.069	-1.000	0.041	0.038	0.003	0.009	-0.889	0.002
1774	-4907000	1.54x10 ⁶	-0.385	-0.294	1.167	-0.853	0.063	0.163	0.000	-0.034	-1.000	0.020
1900	-3748000	1.32x10 ⁶	0.031	-1.000	-0.062	0.556	-0.026	1.563	0.000	-0.016	-0.623	-0.344

Eigenvector 4:



Temp- erature (K)	γ_4 (/s)	c_4 mole/m ³ s	CO	CH ₃ OH	CH ₂ O	O ₂	CH ₄	H ₂	H ₂ O ₂	HO ₂	CO ₂	H ₂ O
1008	-18.1	148.6	-1.000	-0.192	-0.025	-0.727	0.007	0.145	0.000	0.000	1.210	0.249
1028	-67.6	523.6	-1.000	-0.096	-0.012	-0.655	0.011	-0.042	0.001	0.000	1.096	0.222
1048	-176.9	1885	-1.000	-0.075	-0.010	-0.600	0.015	-0.016	0.002	0.000	1.069	0.141
1071	-394.0	5448	-1.000	-0.058	-0.008	-0.565	0.018	-0.008	0.003	0.000	1.048	0.093
1088	-655.8	10 500	-1.000	-0.046	-0.007	-0.542	0.019	-0.007	0.003	0.000	1.034	0.061
1097	-828.8	14 100	-1.000	-0.040	-0.007	-0.532	0.019	0.000	0.004	0.000	1.028	0.047
1130	-1744	34 100	-1.000	-0.023	-0.005	-0.501	0.020	0.006	0.004	0.000	1.009	0.003
1165	-3356	71 600	-1.000	-0.009	-0.002	-0.474	0.019	0.013	0.004	0.000	0.992	-0.035
1169	-3 617	77 900	-1.000	-0.007	-0.002	-0.471	0.019	0.014	0.004	0.001	0.990	-0.040
1294	-18 490	426 000	-1.000	0.024	0.000	-0.414	0.000	0.033	0.000	0.000	0.954	-0.121
1406	-39 640	824 000	-1.000	0.037	0.014	-0.390	0.000	0.053	0.000	0.000	0.941	-0.160
1548	-64 740	1 120000	-1.000	0.053	0.024	-0.344	0.000	0.100	0.000	0.000	0.920	-0.238
1689	-106 700	1 642000	-1.000	0.046	0.025	-0.386	0.000	0.123	0.000	0.000	0.949	-0.202
Temp- erature (K)	γ_4 (/s)	c_4 mole/m ³ s	CO	CH ₃ OH	CH ₂ O	O ₂	OH	H ₂	O	H	CO ₂	H ₂ O
1774	-175 400	2 940000	-1.000	0.047	0.034	-0.291	-0.002	0.147	0.000	0.000	0.903	-0.306
1900	-4331000	7 220000	-1.000	0.018	0.019	-0.372	-0.008	0.000	-0.003	0.000	0.955	-0.190
2096	-2343000	3.21x10 ⁷	-1.000	0.000	0.000	-0.474	-0.096	-0.038	-0.147	-0.031	1.000	0.104
2314	-2880000	2.25x10 ⁷	-1.000	0.000	0.000	-0.452	-0.350	-0.190	-0.159	-0.114	1.000	0.427
2519	-582 900	333 000	-1.000	0.000	0.000	-0.453	-0.490	-0.241	-0.121	-0.069	1.000	0.523
2553	-30 940	14 300	-1.000	0.000	0.000	-0.427	-0.606	-0.248	-0.114	-0.054	1.000	0.580

Eigenvector 5



Temp- erature (K)	γ_5	c_5	CO	O ₂	OH	H ₂	O	H	CO ₂	H ₂ O
2096	-4 395 000	1.35x10 ⁷	1.000	0.419	0.281	0.088	0.136	0.082	-1.000	-0.274
2314	-3 664 000	1.33x10 ⁷	1.000	0.408	0.608	0.313	0.273	0.191	-1.000	-0.719
2519	-2 808 000	19 600	-0.781	-0.635	1.196	0.339	0.281	1.196	0.781	-1.000
2553	-2 125 000	983.0	-0.936	-0.788	1.382	0.267	0.250	0.078	0.936	-1.000

References

1. V.I. Arnold, Ch. *Systems of Linear Differential Equations*, in *Ordinary Differential Equations*, MIT Press (1987).
2. A. Jeffrey, Ch *Linear Systems*, in *Linear Algebra and Ordinary Differential Equations*, Blackwell Scientific (1990).
3. K. Chinnick, C. Gibson, J. Griffiths, W. Kordylewski, *Isothermal Interpretations of Oscillatory Ignition During Hydrogen Oxidation in an Open System. I. Analytical Predictions and Experimental Measurements of Periodicity*, Proc. Royal Soc. London A 405 (1986) 117 – 128.
4. U. Maas, S.B. Pope, *Simplifying chemical kinetics: Intrinsic low-dimensional manifolds in composition space*, Combust. Flame 88 (1992) 239 – 264.
5. U. Maas, S.B. Pope, *Implementation of simplified chemical kinetics based on intrinsic low-dimensional manifolds*, Proc. Combust. Inst. 24 (1992) 103 – 112.
6. U. Maas, S.B. Pope, *Laminar flame calculations using simplified chemical kinetics based on intrinsic low dimensional manifolds*, Proc. Combust. Inst. 25 (1994) 1349 – 1356.
7. H. Bongers, J.A. Van Oijen, L.P.H. De Goeij, *Intrinsic low-dimensional manifold method extended with diffusion*, Proc. Combust. Inst. 29 (2002) 1371 – 1378.

8. V. Bykov, U. Maas, *Extension of the ILDM method to the domain of slow chemistry*, Proc. Combust. Inst. 31 (2007) 465 – 472.
9. S.H. Lam, D.A. Goussis, *Understanding complex chemical kinetics with computational singular perturbation*, Proc. Combust. Inst. 22 (1988) 931 – 941.
10. S.H. Lam, *Using CSP to understand complex chemical kinetics*, Combust. Sc. Tech. 89 (1993) 375 – 404.
11. S.H. Lam, D.A. Goussis, *The CSP method for simplifying chemical kinetics*, Intl. J. Chem. Kin. 26 (1994) 461 – 486.
12. A. Massias, D. Diamantis, E. Mastorakos, D.A. Goussis, *An algorithm for the construction of global reduced mechanisms for CSP data*, Combust. Flame 117 (1999) 685 – 708.
13. T. Lu, Y. Ju, C.K. Law, *Complex CSP for chemistry reduction and analysis*, Combust. Flame 126 (2001) 1445 – 1455.
14. J.C. Lee, H.N. Najm, S. Lefantz, J. Ray, M. Frenklach, M. Valorani, D.A. Goussis, *A CSP and tabulation-based adaptive chemistry model*, Combust. Th. Model. 11 (2007) 73 – 102.

15. R.D. Lockett, *CARS Temperature Measurements and Chemical Kinetic Modelling of Auto-ignition in a Methanol Fuelled Internal Combustion Engine*, PhD Thesis, University of Cape Town (1992) 205 – 247.
16. R.A. Strehlow, Ch. *Flames in Combustion Fundamentals*, McGraw-Hill International Edition (1985).
17. A. Liñan, F.A. Williams, *Fundamental Aspects of Combustion*, Oxford University Press (1993).
18. D.W. Mikolaitis, *An asymptotic analysis of the induction phases of hydrogen-air detonations*, *Combust. Sc. Tech.* 52 (1987) 293 – 323.
19. S. Ghosal, L. Vervisch, *Theoretical and numerical study of a symmetrical triple flame using the parabolic flame path approximation*, *J. Fluid Mech.* 415 (2000) 227 – 260.
20. A.G. Class, B.J. Matkowsky, A.Y. Klimenko, *A unified model of flames as gasdynamic discontinuities*, *J. Fluid Mech.* 491 (2003) 11 – 49.
21. H.S.T. Driver, R.J. Hutcheon, R.D. Lockett, G.N. Robertson, H.H. Grotheer, S. Kelm, *Elementary Reactions in the Methanol Oxidation System. Part II: Measurement and Modeling of Autoignition in a Methanol-Fuelled Otto Engine*, *Berichte der Bunsengesellschaft Phys. Chem. Chem. Phys.* 96 (1992) 1376 – 1387.

22. D. Ball, H.S.T. Driver, R.J. Hutcheon, R.D. Lockett, G.N. Robertson, *CARS temperature measurements in an internal combustion engine*, Opt. Eng. 33 (1994) 2870 – 2874
23. H.H. Grotheer, S. Kelm, H.S.T. Driver, R.J. Hutcheon, R.D. Lockett, G.N. Robertson, *Elementary Reactions in the Methanol Oxidation System. Part I: Establishment of the Mechanism and Modeling of Laminar Burning Velocities*, Berichte der Bunsengesellschaft Phys. Chem. Chem. Phys. 96 (1992) 1360 – 1375.
24. F. Williams, Ch. *Appendix B – Review of Chemical Kinetics in Combustion Theory (Second Edition)*, Perseus Books (1985).
25. K.K. Kuo, Ch. *Review of Chemical Kinetics in Principles of Combustion*, John Wiley and Sons (1986).
26. J. Warnatz, U. Maas, R.W. Dibble, Ch. *Analysis of Reaction Mechanisms in Combustion (3rd Edition)*, Springer (2001).
27. R.A. Yetter, F.L. Dryer, and H. Rabitz, *Some Interpretive Aspects of Elementary Sensitivity Gradients in Combustion Kinetics Modeling*, Combust. Flame 59 (1985) 107.
28. J. Warnatz, HOMREACT, <http://reaflow.iwr.uni-heidelberg.de/software/> (2006).

29. P. Deuflhard, U. Nowak, University of Heidelberg, Technical Report 332 (1985).
30. T. Norton, F. Dryer, *Some new observations on methanol oxidation chemistry*, Combust. Sc. Tech. 63 (1989) 107 – 129.
31. T.J. Held, F.L. Dryer, *A comprehensive mechanism for methanol oxidation*, Int. J. Chem. Kin. 30 (11) (1998) 805 – 830.

List of Tables

Table 1: A Table of Species and Reactions Showing the Local Reaction Flow Analysis.

List of Figures

Figure 1: Integrated reaction path describing the oxidation of methanol in air.

Figure 2: Histogram showing normalized sensitivities of species concentrations to the reaction $\text{H}_2\text{O}_2 + \text{M} \rightarrow \text{OH} + \text{OH} + \text{M}$ in the auto-ignition of methanol in air (determined at 1250 K).

Figure 3: Graph of Major Species Concentrations and Temperature versus Time for the Auto-ignition of Methanol and Air.

Figure 4: Graph of Intermediate Species Concentrations and Temperature versus Time for the Auto-ignition of Methanol and Air.

Figure 5: Graph of Dominant Eigen-mode Rates of Formation versus Temperature during the Auto-ignition of Methanol and Air.

Figure 6: Graph of the Dominant Eigen-mode Eigenvalue versus Temperature during the Auto-ignition of Methanol and Air (Describing Methanol Oxidation).

Figure 7: Graph of the Secondary Eigen-mode Eigenvalues versus Temperature during the Auto-ignition of Methanol and Air.

Reaction	Species→							
↓	1	2	3	4	5	M - 1	M
1	-15%	-3%	0	0	0		0	0
2	0	0	-10%	-20%	0		0	0
3	0	0	-8%	-6%	0		4%	5%
.								
.								
N - 1	0	-40%	-40%	0	0		20%	25%
N	0	0	-2%	0	-3%		2%	2%

Table 1: A Table of Species and Reactions Showing a Local Reaction Flow Analysis.

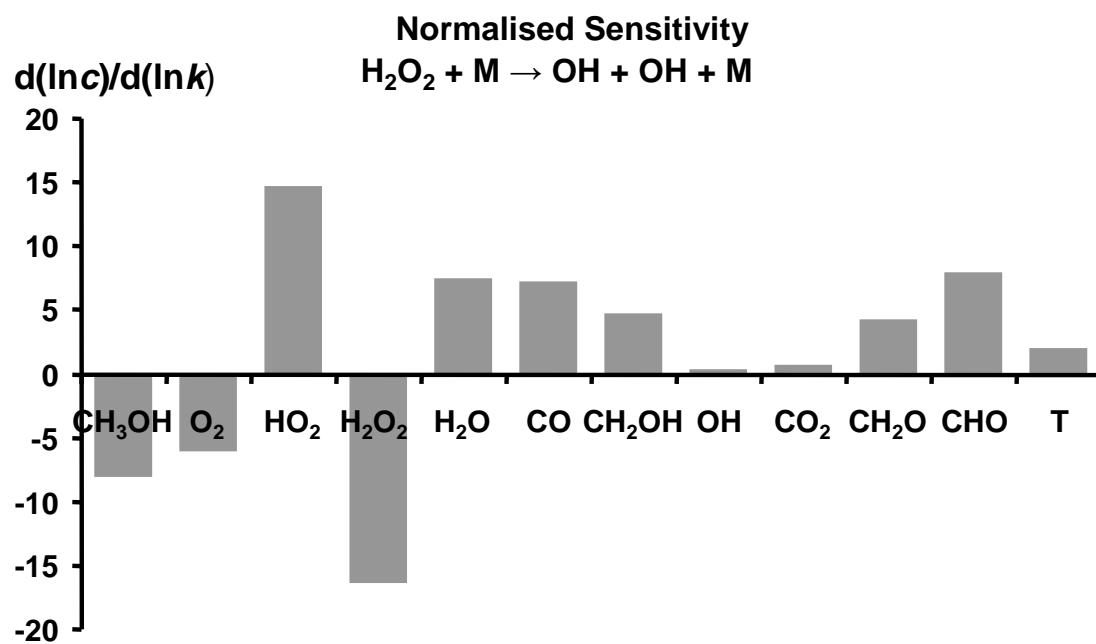


Figure 2: Histogram showing normalized sensitivities of species concentrations to the reaction $\text{H}_2\text{O}_2 + \text{M} \rightarrow \text{OH} + \text{OH} + \text{M}$ in the auto-ignition of methanol in air (determined at 1250 K).

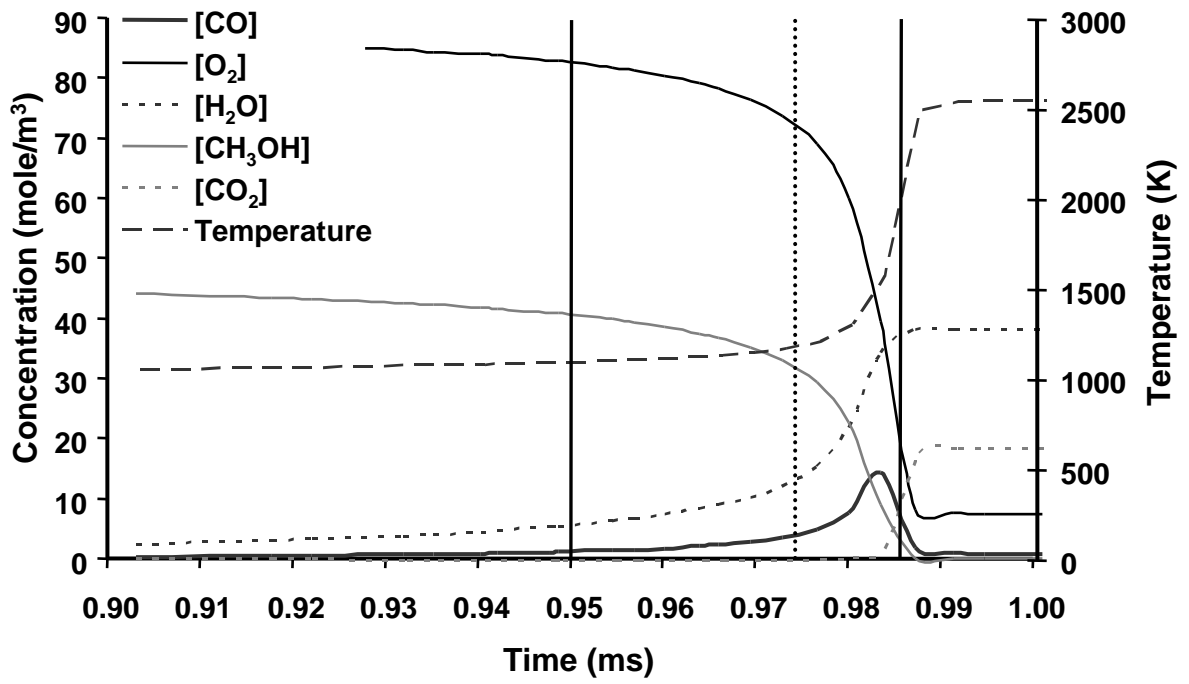


Figure 3: Graph of Major Species Concentrations and Temperature versus Time for the Auto-ignition of Methanol and Air.

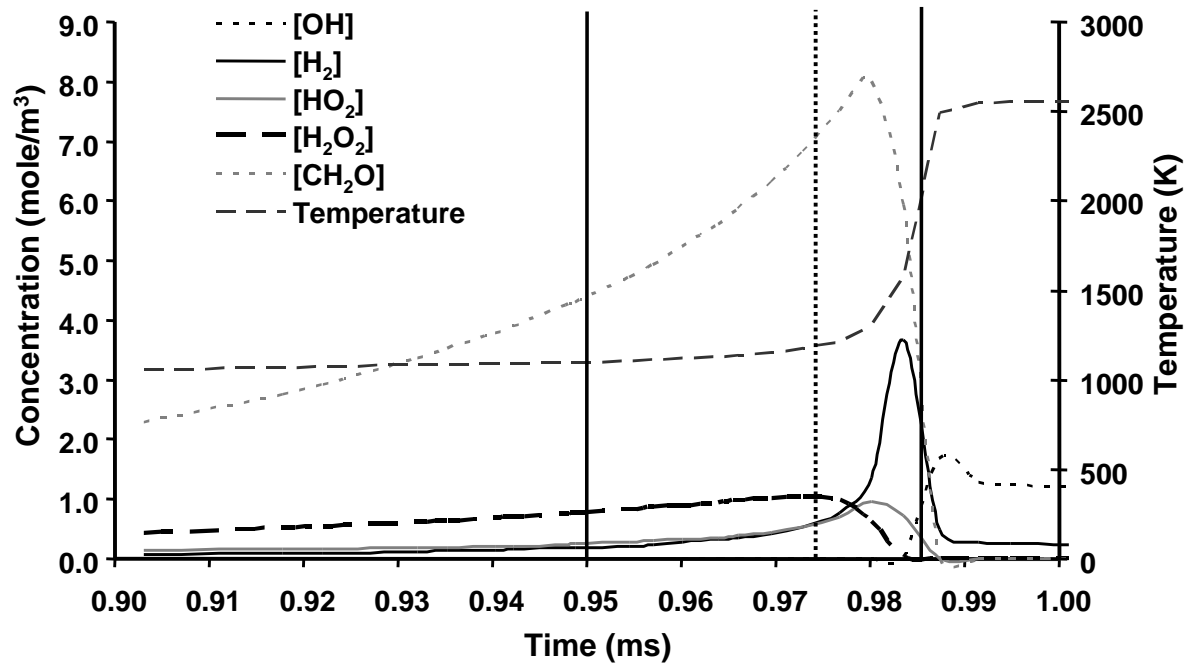


Figure 4: Graph of Intermediate Species Concentrations and Temperature versus Time for the Auto-ignition of Methanol and Air.

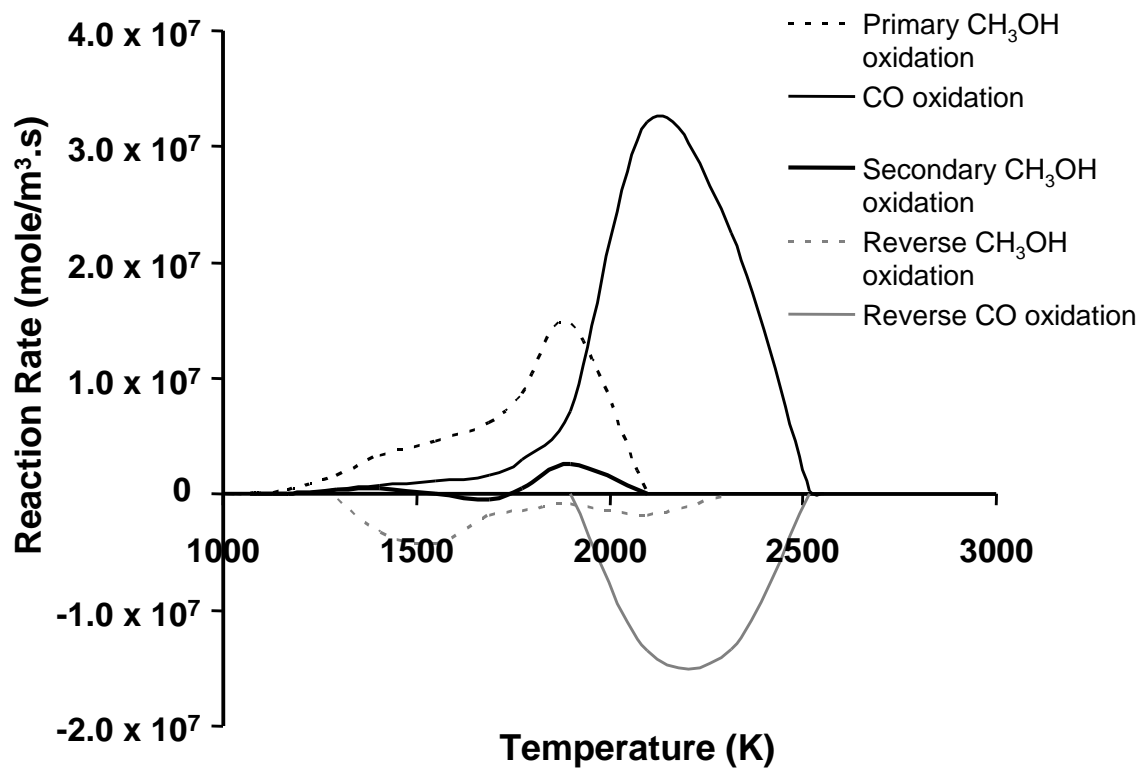


Figure 5: Graph of Dominant Eigen-mode Rates of Formation versus Temperature during the Auto-ignition of Methanol and Air.

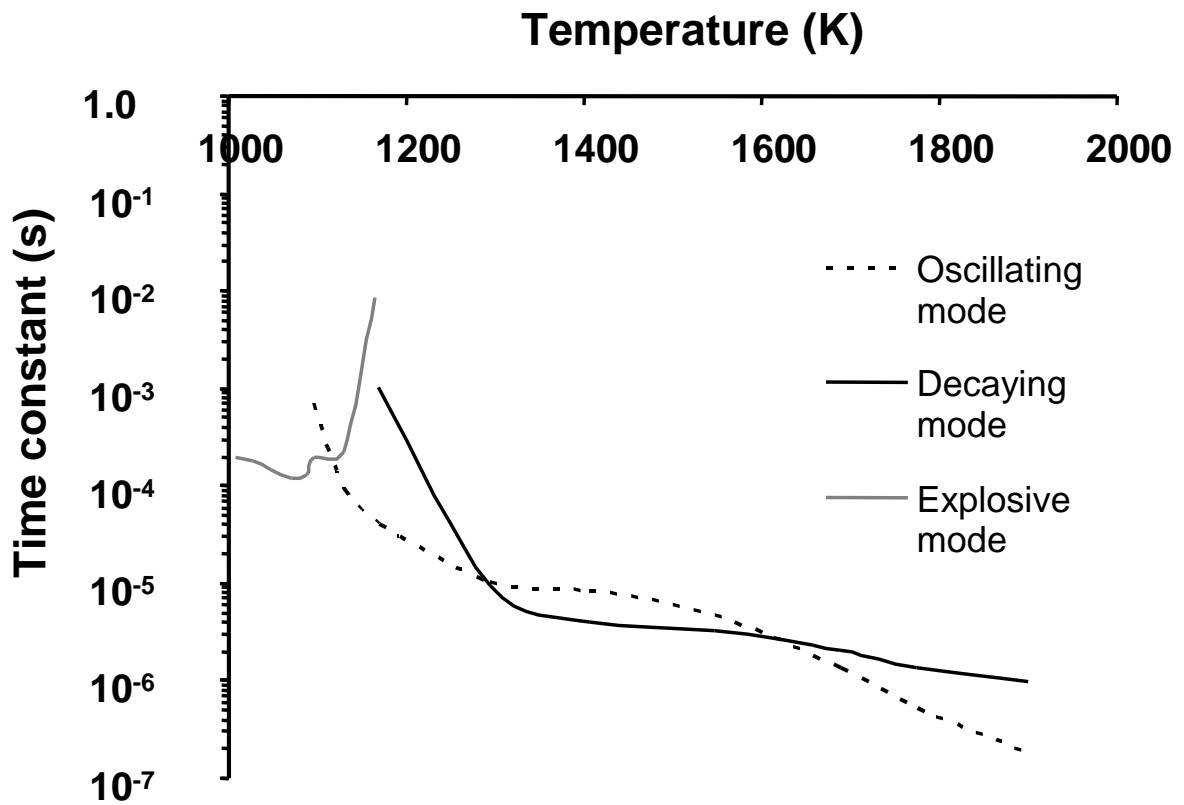


Figure 6: Graph of the Dominant Eigen-mode Eigenvalue versus Temperature during the Auto-ignition of Methanol and Air (Describing Methanol Oxidation).

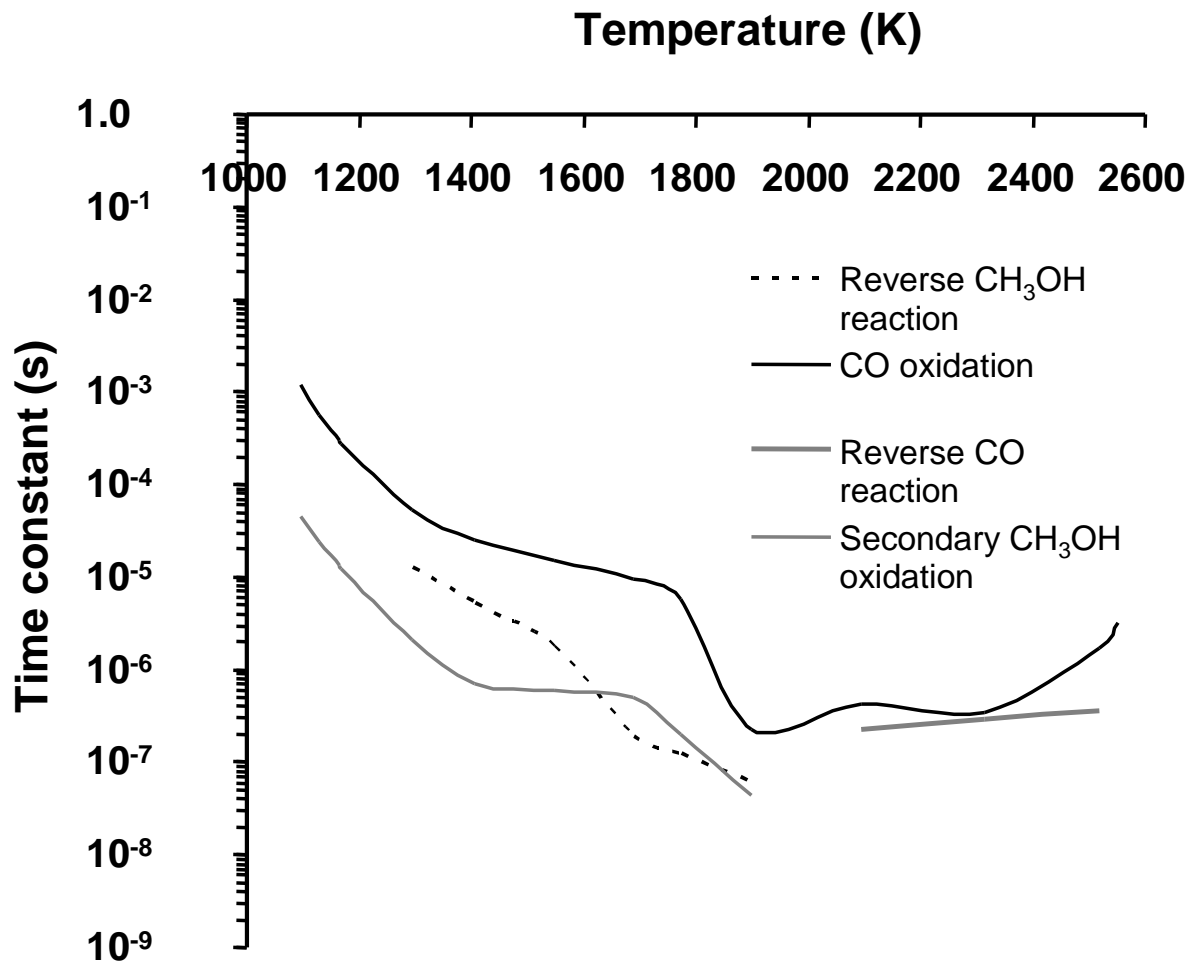


Figure 7: Graph of the Secondary Eigen-mode Eigenvalues versus Temperature during the Auto-ignition of Methanol and Air.